

A CRISPR-Cas12a-based specific enhancer for more sensitive detection of SARS-CoV-2 infection

Weiren Huang^{1†}, Lei Yu^{1†}, Donghua Wen^{2†}, Dong Wei^{3†}, Yangyang Sun^{1†}, Huailong Zhao⁴, Yu Ye⁵, Wei Chen¹, Yongqiang Zhu⁶, Lijun Wang⁶, Li Wang⁷, Wenjuan Wu², Qianqian Zhao⁸, Yong Xu¹, Dayong Gu¹, Guohui Nie¹, Dongyi Zhu², Zhongliang Guo², Xiaoling Ma⁹, Liman Niu¹, Yikun Huang¹, Yuchen Liu¹, Bo Peng¹⁰, Renli Zhang¹⁰, Xiuming Zhang¹¹, Dechang Li¹², Yang Liu¹³, Guoliang Yang⁴, Lanzheng Liu⁴, Yunying Zhou⁸, Yunshan Wang⁸, Tieying Hou¹⁴, Qiuping Gao¹⁵, Wujiao Li¹, Shuo Chen⁵, Xuejiao Hu¹⁴, Mei Han¹⁶, Huajun Zheng⁶, Jianping Weng⁹, Zhiming Cai¹, Xinxin Zhang³, Fei Song^{1*}, Guoping Zhao^{15, 17, 18*}, Jin Wang^{19*}

Affiliations:

¹Department of Urology, Shenzhen Second People's Hospital, The First Affiliated Hospital of Shenzhen University, International Cancer Center, Shenzhen University School of Medicine, Shenzhen 518039, China

²Department of Laboratory Medicine, Shanghai East Hospital, Tongji University School of Medicine, Shanghai 200123, China

³Research Laboratory of Clinical Virology, Ruijin Hospital, Shanghai Jiaotong University School of Medicine, Shanghai 200025, China

⁴Jinan Center for Disease Control and Prevention, Jinan, Shandong 250021, China

⁵Shenzhen Institute of Synthetic Biology, Shenzhen Institutes of Advanced Technology, Chinese Academy of Sciences, Shenzhen 518055, China

⁶Shanghai-MOST Key Laboratory of Health and Disease Genomics, Chinese National Human Genome Center at Shanghai, Shanghai, 201203, China

⁷Jinan Infectious Diseases Hospital of Shandong University, Jinan, Shandong 250021, China

⁸Medical Research & Laboratory Diagnostic Center, Jinan Central Hospital Affiliated to Shandong University, Jinan, Shandong 250013, China

⁹The First Affiliated Hospital of USTC, Division of Life Sciences and Medicine, University of Science and Technology of China, Hefei, Anhui 230001, China

¹⁰Shenzhen Center for Disease Control and Prevention, Shenzhen 518055, China

¹¹Shenzhen Sixth People's Hospital (Nanshan Hospital), Huazhong University of Science and Technology Union Shenzhen Hospital, Shenzhen 518052, China

¹²Yuebei Second People's Hospital, Shaoguan, Guangdong 512000, China

¹³Shanghai Institute of Quality Inspection and Technical Research/National Quality Supervision and Inspection Center for Food Products (Shanghai), Shanghai 200233, China

¹⁴Laboratory of Medicine, Provincial People's Hospital, Guangdong Academy of Medical Sciences Guangzhou, Guangdong 510080, China

¹⁵Tolo Biotechnology Company Limited, Shanghai 200233, China

¹⁶Public Health Medical Centre of Chongqing Municipality, Chongqing 400036, China

¹⁷CAS Key Laboratory of Synthetic Biology, Institute of Plant Physiology and Ecology,
Shanghai Institutes for Biological Sciences, Chinese Academy of Sciences, Shanghai 200032,
China

¹⁸Bio-Med Big Data Center, Key Laboratory of Computational Biology, CAS-MPG Partner
Institute for Computational Biology, Shanghai Institute of Nutrition and Health, Chinese
Academy of Sciences, Shanghai 200031, China

¹⁹College of Life Sciences, Shanghai Normal University, Shanghai 200234, China

*Correspondence to: F. S., lst121@outlook.com; G.Z., gpzhao@sibs.ac.cn; J.W.,
wangj01@hotmail.com.

†These authors contributed equally to this work.

One Sentence Summary: CRISPR-Cas12a-based COVID-19 diagnosis.

Abstract:

High Ct-values falling in the grey zone are frequently encountered in SARS-CoV-2 detection by real-time reverse transcription PCR (rRT-PCR) and have brought urgent challenges in diagnosis of samples with low viral load. Based on the single-stranded DNA reporter *trans*-cleavage activity by Cas12a upon target DNA recognition, we create a Specific Enhancer for detection of PCR-amplified Nucleic Aacids (SENA) to confirm SARS-CoV-2 detection through specifically targeting its rRT-PCR amplicons. SENA is highly sensitive, with its limit of detection being at least 2 copies/reaction lower than that of the corresponding rRT-PCR, and highly specific, which identifies both false-negative and false-positive cases in clinic applications. SENA provides effective confirmation for nucleic acid amplification-based molecular diagnosis, and may immediately eliminate the uncertainty problems of rRT-PCR in SARS-CoV-2 clinic detection.

Key words: COVID-19, SARS-CoV-2, rRT-PCR, CRISPR diagnosis, Cas12a, SENA

Main Text:

Since December 2019, the outbreak of COVID-19, caused by the infection of the SARS-CoV-2, has rapidly spread throughout the world (1), and is now a global pandemic. Till June 1, 2020, the outbreak has affected 216 countries, areas and territories, infected 6 million people, and caused more than 370 thousand of death (2). One of the greatest public health concerns in combating against the pandemic is a prompt response to meet the urgent demand for rapid and accurate diagnosis of the virus. Currently, nucleic acid amplification-based molecular diagnostics (MDx) is the most accurate, fast and affordable and thus the preferred method for diagnosis of SARS-CoV-2 infection, and the real-time reverse transcription PCR (rRT-PCR) kits have been successfully developed by quite a few laboratories and commercial companies (3). However, since its clinical application at least five months ago in China, the diagnostic performance of rRT-PCR for SARS-CoV-2 has brought some urgent challenges, particularly with the frequently encountered high Ct-value designated “grey zone” associated uncertain negative or positive readouts (4-8). Besides of “human error” factors such as misconducted sampling, unqualified reagents and uncalibrated diagnostic equipment, inefficient RT reaction and PCR amplification of clinical samples with very low viral loads are likely the major intrinsic causative factors for the fuzzy rRT-PCR readouts and uncertain diagnosis. Although repetitive sampling and assays are implemented for final confirmation of the diagnosis, these “trouble shooting” efforts are time-consuming and may still fail to detect the low viral load samples from some mild or asymptomatic patients, or from the recovering patients, resulting in false-negative diagnosis that may cause serious public concerns in battling against the pandemic (**Figure 1**).

With the characterization of non-specific *trans*-cleavage activities against single-stranded nucleic acids in several CRISPR-associated (Cas) proteins, *e.g.*, Cas12, Cas13 and Cas14 (9-15), Clustered Regularly Interspaced Short Palindromic Repeats Diagnostics (CRISPR-Dx) technology (16, 17) was established and has been developing rapidly. The underline mechanism for CRISPR-Dx, as illustrated by the Cas12a-based HOLMES system for example (18), is based on the efficient *trans*-cleavage activity against a fluorophore quencher (FQ)-labeled single-stranded DNA reporter by Cas12a triggered upon target DNA recognition, which is guided by a specific CRISPR RNA (crRNA), generating exponentially increasing fluorescence signal within several minutes. With this mechanism, here, we design a Specific Enhancer for detection of PCR-amplified Nucleic Aacids (SENA) to improve both the detection sensitivity and specificity against the pre-amplified targeted SARS-CoV-2 genomic fragments (**Figure 1**). Briefly, the COVID-19 clinic samples are firstly analyzed by the well-established rRT-PCR assays and amplicons with uncertain readouts are then verified by SENA in a physically isolated space, avoiding contamination of the PCR laboratory during pipetting.

To prepare appropriate crRNAs for SENA detection, we firstly determined the amplicon sequences from several commercial rRT-PCR kits used in China and then designed specific crRNAs corresponding to each of the distinct amplicons (**Table S1**). Candidate crRNAs were prepared and analyzed in a SENA system comprised of Cas12a, crRNAs, FQ-reporter and the rRT-PCR products using templates of either the positive or negative controls, and the best crRNAs, *i.e.*, the lowest fluorescence with the negative control and highest with the positive control, were chosen for further SENA assays (data not shown). If a kit detects more than one gene, *e.g.*, Orf1ab (“abbreviated as *O*”), *E* and *N* genes, corresponding crRNAs were mixed in a SENA system to enhance the detection signal.

The performance of SENA was quantitatively characterized *via* a systematic titration upon rRT-PCR amplicons employing pure SARS-CoV-2 RNA standards comprised of the *O* and *N* fragments as the templates. As it is aware that the viral nucleic acids extracted from patients' samples such as nasopharyngeal swabs usually contain some biological and chemical contaminants that might inhibit the enzyme activities for reverse transcription and PCR reactions (19) and is likely one of the causal effects attributed to the low efficiency of rRT-PCR in clinical analysis. In order to mimic the clinical sampling for the titration experimentation, the RNA standards were serially diluted in buffer prepared by mixing the nucleic acid extracts from 40 COVID-19 negative people, generating RNA templates ranging from 0.025 to 25 copies per reaction (Rx).

Due to the Poisson distribution property of sampling, replica variations become extremely significant when the template copies in individual reaction are designed to be low, *i.e.*, less than 3-4 copies/Rx, near the limit of detection (LoD) for rRT-PCR (20, 21), and extremely low, *i.e.*, equal to and less than 1 copy/Rx. To overcome this sampling ambiguity problem, we performed 9 replicas for groups with 1 and 0.5 RNA template copies/Rx while 6 replicas for each of the rest concentrations. In addition, although the rRT-PCR assay supplier, Shanghai BioGerm (BJ), who follows the Chinese CDC recommended primer sets (**Table S1**), recommends 40 cycles of PCR amplification, we set 45 cycles as routine aiming at recording maximum exact Ct values if possible. After rRT-PCR reaction, all amplicons were subjected to 3 individual SENA reactions, *i.e.*, N-SENA, O-SENA and mix-SENA with crRNAs targeting *O* gene, *N* gene and both, respectively.

Consistent with the theoretical analysis (20) and rigorous experimentation (21), along with the decrease of the RNA templates to less than 3 copies/Rx, the rRT-PCR Ct values in some replicas, primarily that corresponding to the *N* gene, passed 38 (the cut-off for positive as recommended by the rRT-PCR kit suppliers) but were less than 40, which should be considered as entering the "grey zone". The Ct values increased steadily when the concentration of the RNA templates further decreased, with more and more replicas showing one or both Ct values entering the "grey zone" and eventually all became "negative", *i.e.*, greater than 40 or even 45 (**Figure 2A, Table S2 and Figure S1**). Employing Ct=38 as the cut-off for "positive" detection, we estimated the LoD for *O* and *N* genes with 95% confidence interval (CI) of this set of rRT-PCR assay as $3.3 \leq 4.0 \leq 6.1$ and $4.0 \leq 4.1 \leq 4.4$, respectively (**Figure S2**). Most likely due to the influence of the complex combination of the targeted viral genomic fragments and the clinic sampling background, the LoD determined in this study was clearly higher than the published value of $2.0 \leq 2.5 \leq 3.7$, which analyzed single target in a pure system (21).

The rRT-PCR amplicons were further analyzed by SENA detection with the measurement of the fluorescence signals for each corresponding replica. After comparison of the parameters of slope (increase of fluorescence/min) versus FC (the fold of change of fluorescence between that of the sample over that of the negative control at certain time point), we defined a parameter, *FCratio*, which is the ratio of the FC at 10 min to that at 5 min after the initiation of fluorescence reading (**Figure S1 and Table S2**). We also found that in the cases with low concentrations of templates, the rRT-PCR efficiency of the two target genes (*i.e.*, *O* and *N*) were different so as the SENA detection (**Figures S1 and S2**). In order to verify the existence of specific amplicons of SARS-CoV-2 nucleic acids in an individual rRT-PCR reaction, all of the amplicons of the replicas with RNA templates ranging from 0.125 to 2 copies/Rx were subjected to next generation sequencing (NGS) analysis. The results were found to be completely consistent with the perspective results of both O-SENA and mix-SENA. In addition, with mix-SENA, not only the signals are generally more significant than that of the O-SENA detection but also may resolve

some of the ambiguity readouts found with N-SENA (**Figure S1** and **Table S2**). Based on these results, the mixFCratio was demonstrated as the most sure-proof index for rRT-PCR confirmation, and we empirically estimated that $\text{mixFCratio} \geq 1.145$ for positive cut-off, and $\text{mixFCratio} \leq 1.020$ for negative cut-off (**Figure 2A**). Of course, these two parameters are subject to further verification and adjustment along with the increase of tested samples. Because SENA is rRT-PCR based, the same methodology for determining the rRT-PCR LoD was used to estimate that of SENA by this set of data, corresponding to both individual *O* and *N* fragments (**Figure S2**) and in combination as indicated by the mix-SENA (**Figure 2B**). As expected, the N-SENA LoD ($3.7 \leq 4.3 \leq 4.8$ with 95% CI) is very close to that of the N-Ct of rRT-PCR, while the LoD of O-SENA ($1.1 \leq 1.3 \leq 1.7$ with 95% CI) is significantly lower than that of O-Ct (**Figure S2**). Although the LoD of mix-SENA ($1.2 \leq 1.6 \leq 2.1$ with 95% CI) is slightly higher than that of O-SENA (**Figure 2B and Figure S2**), it is apparently caused by its capable of confirming some of the ambiguous amplicons in the extremely low concentration cases (**Figure S2**) and thus, mixFCratio is chosen for clinic applications.

SENA was further verified in a few hospitals, testing various clinic specimens and samples under different scenarios (**Figure 1**) and employing few more commercial rRT-PCR diagnosis kits in addition to BJ which was used in the titration experiment (**Table S1**). Totally 295 clinic samples or specimens (mainly pharyngeal swabs) collected from 282 individuals were tested by rRT-PCR followed by SENA detection (**Table S3**). Except for asymptomatic carriers, all the cases of uncertain analytic and false positive or negative readouts of rRT-PCR diagnosis were encountered and finally confirmed or corrected by SENA detection.

Specifically, samples from 139 patients of Ruijin Hospital (RJ, Shanghai, China) were assayed by rRT-PCR employing diagnostic kits of ZJ and HD, 137 of which had consistent readouts by both rRT-PCR kits, indicating two positive, 123 negative and 12 suspected that fell in the “grey zone” (**Table S3**). SENA detection of these samples revealed not only the 12 suspected as negative but also identified one more positive among the original 123 negative individuals, clearly a case of false negative diagnosis (**Table S3**). Besides, distinct rRT-PCR assay results, positive by HD but negative by ZJ were shown for samples collected from 2 close contacts of COVID-19 patients and apparently asymptomatic (ref to **Table S3**). However, the amplicons of both ZJ and HD were shown as negative via SENA detection. All these ambiguous rRT-PCR amplicons (17 samples, ref to **Table S3**) were finally analyzed by NGS, and the results were consistent with the SENA. Noticeably, the rRT-PCR false-negative COVID-19 patient was symptomatically mild at the point of admission with all the clinic laboratory tests negative but turned positive after 24 hours. On the other hand, although those 12 suspected patients had respiratory infection symptoms, they were finally excluded from COVID-19 according to the latest guideline for diagnosis and treatment from China National Health commission (the 6th edition). Similarly, in Shenzhen Second People's Hospital (SZII, Shenzhen, China), 5 uncertain rRT-PCR readouts for *O* gene were found among 139 individuals. Three of them had Ct value of 39.47, 39.7 and 40.56, respectively but the following SENA detection gave mixFCratio values less than 1.0 for all of them, indicating all negative. The other two individuals had Ct values of 38.87 and 39.22, while their mixFCratio values were 1.581 and 1.609, respectively, indicating positive for both. In addition, there were another three individuals with Ct values larger than 40 for *O* gene and 36.09, 35.88 and 37.98 for *N* gene, respectively; however, the following SENA detection showed mixFCratio values were 1.39, 1.55 and 1.21, respectively, indicating all positive. All these amplicons were further confirmed by NGS analysis (**Table S3**), obtaining consistent results with those of SENA.

Consistently, the three SENA-negative individuals were finally excluded from SARS-CoV-2 infection after being rechecked by rRT-PCR after 24 hours (**Table S3**). Based on above data, it is clear, SARS-CoV-2 infection suspects with either rRT-PCR Ct values falling in the “grey zone” or with clear patient-contact epidemiological history but negative rRT-PCR tests, are strongly recommended to perform SENA detection to minimize the possibility of misdiagnosis. On the other hand, in case an rRT-PCR-positive suspect does not demonstrate any COVID-19 clinic symptoms and/or signs, SENA detection is also strongly recommended to eliminate either false-positive diagnosis or misdiagnosis of the so-called “asymptomatic carrier” or “asymptomatic patient”.

Besides of preventing false-negative or false-positive diagnosis, the highly sensitive property of SENA may also assist in providing evidence of viral clearance for COVID-19 recovering patients. A female patient in Dongfang Hospital (DF, Shanghai, China) was confirmed as COVID-19 positive by both rRT-PCR and CT scanning and showed ground-glass opacities mixed with consolidation along the subpleural area (**Figure 3**). Accordingly, the SENA test was positive with the $mixFCratio$ of 1.43. After the hospitalization, the patient was further analyzed by rRT-PCR at two time points, obtaining all negative results with bilateral nasal and pharyngeal swab specimens. However, the $mixFCratios$ of SENA for some of her specimens were 1.64, 1.36 and 1.00, respectively, indicating that the virus was contained and yet to be cleared. On the sixth day, both rRT-PCR and the corresponding SENA detection for all of her specimens were negative and these results were confirmed by NGS and consistent with her normal CT scanning results (**Figure 3**). Thus, she was discharged from the hospital and safely back to home. Similar cases were found in Jinan of Shandong Province, China, where the fecal samples from two recovering COVID-19 patients were tested negative by rRT-PCR but clearly positive by SENA (**Table S3**). Considering a certain percentage of the recovered patients discharged from hospitals were reported to be re-detectable positive (RP) (22), the incomplete clearance of the SARS-CoV-2 virus ahead of discharge might be one of the possible causes. Therefore, it could be necessary to consider more sensitive detection approaches such as SENA as a potential index of viral clearance.

To reconfirm and/or improve the cut-off values for SENA $mixFCratio$, the ambiguous Ct values were re-estimated using the regression functions derived from the rRT-PCR assays with titrated standard RNA templates (**Figures S4 and S5**), and then the Ct values (both estimated and detected) were plotted against the corresponding $mixFCratios$ (**Figure 4**). Combining the data from both RNA standards and clinic samples, it is clear that SENA detection is of both high sensitivity, identifying real positive samples with Ct values as high as more than 43 (approaching 50 as estimated), and high specificity, identifying real negative samples with Ct values as low as 39. Therefore, SENA can effectively eliminate uncertain diagnosis of rRT-PCR assays for SARS-CoV-2 infection. In addition, the cut-off value for SENA $mixFCratio$ remains unchanged as 1.145 for positive diagnosis while slightly increased to 1.068 for negative (**Figure 4**), which is supposed to further increase along with the clinic applications.

Instead of developing a closed CRISPR-Dx system, which, ideally, should be comprised of both target nucleic acids amplification and CRISPR-Cas-based *trans*-cleavage assays, SENA was created here to match the commercially available and widely applied rRT-PCR kits, and to solve the uncertainty challenge of the rRT-PCR “grey zone” in COVID-19 diagnosis. Although there are dozens of commercial rRT-PCR kits using distinct PCR primers and probes, their corresponding SENA detection kits can be easily designed and prepared following the instructions provided in this study. Considering the fact that qPCR is the most popular MDx system and SENA

is simple to operate, SENA thus has the potential to be widely used in various scenarios to solve the uncertainty problems of qPCR as well as other nucleic acid amplification-based MDx. Of course, to minimize the possibility of aerosol contamination during opening of the PCR tubes and pipetting, physical separation of the SENA detection center from the clinical PCR laboratory is an absolute requisition. Abided by this rule, SENA has been demonstrated convenient and effective in several hospitals and centers for disease control and prevention as part of their laboratory routine in combination with rRT-PCR for more sensitive and accurate detection of SARS-CoV-2 infection. Therefore, SENA is a useful technique that meets the urgent needs of combating COVID-19 pandemic.

Acknowledgments:

We thank Yucai Wang and Linxian Li for discussions and support. J.W. is supported by the National Natural Science Foundation of China (31922046); W.H. is supported by the National Key R&D Program of China (2019YFA0906000) and NSFC (81772737); D.W. is supported by NSFC (81972830) and Shanghai “Rising Stars of Medical Talent” Youth Development Program-Clinical Laboratory Practitioners Program; F.S. is supported by NSFC (31670757); G.Z. is supported by the Strategic Priority Research Program of the Chinese Academy of Sciences (XDB19040200).

Competing interests:

G.Z. and J.W. are cofounders of Tolo Biotechnology Co., Ltd. W.H., G.Z. and J.W. have filed patent applications relating to the work in this manuscript.

Data and materials availability:

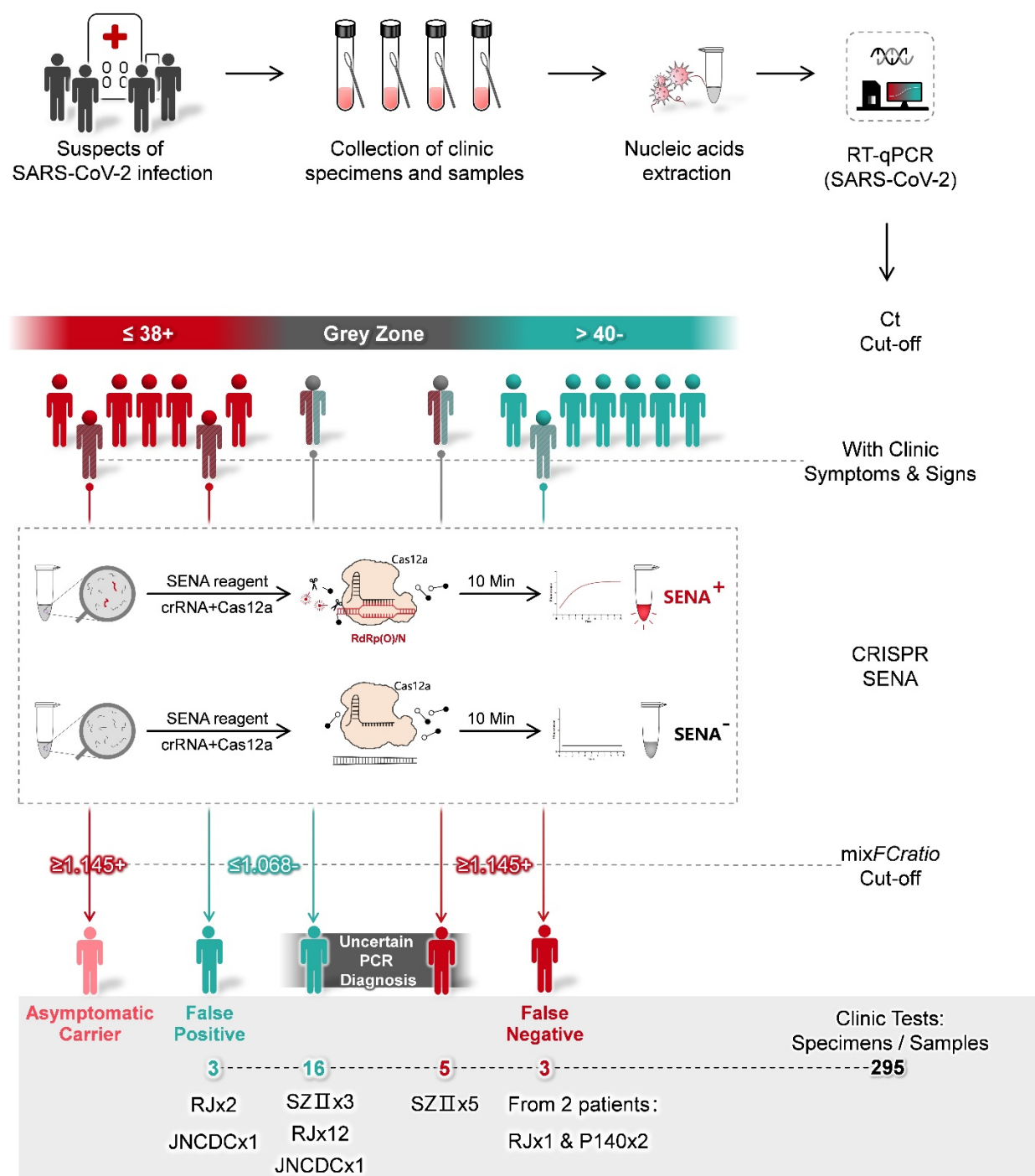
“All data is available in the main text or the supplementary materials.”

References

1. F. Wu, S. Zhao, B. Yu, Y. M. Chen, W. Wang, Z. G. Song, Y. Hu, Z. W. Tao, J. H. Tian, Y. Y. Pei, M. L. Yuan, Y. L. Zhang, F. H. Dai, Y. Liu, Q. M. Wang, J. J. Zheng, L. Xu, E. C. Holmes, Y. Z. Zhang, A new coronavirus associated with human respiratory disease in China. *Nature* **579**, 265-269 (2020). doi: [10.1038/s41586-020-2008-3](https://doi.org/10.1038/s41586-020-2008-3).
2. W. H. Organization, Coronavirus disease 2019 (COVID-19) Situation Report-132. Available at: <https://www.who.int/emergencies/diseases/novel-coronavirus-2019/situation-reports/>. Last accessed, May 31, 2020.
3. V. M. Corman, O. Landt, M. Kaiser, R. Molenkamp, A. Meijer, D. K. Chu, T. Bleicker, S. Brunink, J. Schneider, M. L. Schmidt, D. G. Mulders, B. L. Haagmans, B. van der Veer, S. van den Brink, L. Wijsman, G. Goderski, J. L. Romette, J. Ellis, M. Zambon, M. Peiris, H. Goossens, C. Reusken, M. P. Koopmans, C. Drosten, Detection of 2019 novel coronavirus (2019-nCoV) by real-time RT-PCR. *Euro surveillance*, **25**, (2020). doi: [10.2807/1560-7917.ES.2020.25.3.2000045](https://doi.org/10.2807/1560-7917.ES.2020.25.3.2000045).
4. H. Feng, Y. Liu, M. Lv, J. Zhong, A case report of COVID-19 with false negative RT-PCR test: necessity of chest CT. *Jpn J Radiol*, (2020). doi: [10.1007/s11604-020-00967-9](https://doi.org/10.1007/s11604-020-00967-9).
5. Y. Li, L. Yao, J. Li, L. Chen, Y. Song, Z. Cai, C. Yang, Stability issues of RT-PCR testing of SARS-CoV-2 for hospitalized patients clinically diagnosed with COVID-19. *Journal of medical virology*, (2020). doi: [10.1002/jmv.25786](https://doi.org/10.1002/jmv.25786).
6. Y. Pan, L. Long, D. Zhang, T. Yan, S. Cui, P. Yang, Q. Wang, S. Ren, Potential false-negative nucleic acid testing results for Severe Acute Respiratory Syndrome Coronavirus 2 from thermal inactivation of samples with low viral loads. *Clin Chem*, (2020). doi: [10.1093/clinchem/hvaa091](https://doi.org/10.1093/clinchem/hvaa091).
7. J. Wu, J. Liu, S. Li, Z. Peng, Z. Xiao, X. Wang, R. Yan, J. Luo, Detection and analysis of nucleic acid in various biological samples of COVID-19 patients. *Travel medicine and infectious disease*, 101673 (2020). doi: [10.1016/j.tmaid.2020.101673](https://doi.org/10.1016/j.tmaid.2020.101673).
8. A. T. Xiao, Y. X. Tong, S. Zhang, False-negative of RT-PCR and prolonged nucleic acid conversion in COVID-19: Rather than recurrence. *Journal of medical virology*, (2020). doi: [10.1002/jmv.25855](https://doi.org/10.1002/jmv.25855).
9. J. S. Gootenberg, O. O. Abudayyeh, J. W. Lee, P. Essletzbichler, A. J. Dy, J. Joung, V. Verdine, N. Donghia, N. M. Daringer, C. A. Freije, C. Myhrvold, R. P. Bhattacharyya, J. Livny, A. Regev, E. V. Koonin, D. T. Hung, P. C. Sabeti, J. J. Collins, F. Zhang, Nucleic acid detection with CRISPR-Cas13a/C2c2. *Science* **356**, 438-442 (2017). doi: [10.1126/science.aam9321](https://doi.org/10.1126/science.aam9321).
10. J. S. Gootenberg, O. O. Abudayyeh, M. J. Kellner, J. Joung, J. J. Collins, F. Zhang, Multiplexed and portable nucleic acid detection platform with Cas13, Cas12a, and Csm6. *Science* **360**, 439 (2018). doi: [10.1126/science.aag0179](https://doi.org/10.1126/science.aag0179).
11. S. Y. Li, Q. X. Cheng, J. K. Liu, X. Q. Nie, G. P. Zhao, J. Wang, CRISPR-Cas12a has both cis- and trans-cleavage activities on single-stranded DNA. *Cell research* **28**, 491-493 (2018). doi: [10.1038/s41422-018-0022-x](https://doi.org/10.1038/s41422-018-0022-x).
12. J. S. Chen, E. Ma, L. B. Harrington, M. Da Costa, X. Tian, J. M. Palefsky, J. A. Doudna, CRISPR-Cas12a target binding unleashes indiscriminate single-stranded DNase activity. *Science* **360**, 436-439 (2018). doi: [10.1126/science.aar6245](https://doi.org/10.1126/science.aar6245).
13. L. B. Harrington, D. Burstein, J. S. Chen, D. Paez-Espino, E. Ma, I. P. Witte, J. C. Cofsky, N. C. Kyrpides, J. F. Banfield, J. A. Doudna, Programmed DNA destruction by miniature CRISPR-Cas14 enzymes. *Science* **362**, 839-842 (2018). doi: [10.1126/science.aav4294](https://doi.org/10.1126/science.aav4294).
14. L. Li, S. Li, N. Wu, J. Wu, G. Wang, G. P. Zhao, J. Wang, HOLMESv2: a CRISPR-Cas12b-assisted platform for nucleic acid detection and DNA methylation quantitation. *ACS Synth Biol*, (2019). doi: [10.1021/acssynbio.9b00209](https://doi.org/10.1021/acssynbio.9b00209).
15. D. S. Chertow, Next-generation diagnostics with CRISPR. *Science* **360**, 381-382 (2018). doi: [10.1126/science.aat4982](https://doi.org/10.1126/science.aat4982).
16. G. Gasiunas, R. Barrangou, P. Horvath, V. Siksnys, Cas9-crRNA ribonucleoprotein complex mediates specific DNA cleavage for adaptive immunity in bacteria. *Proceedings of the National Academy of Sciences of the United States of America* **109**, E2579-2586 (2012). doi: [10.1073/pnas.1208507109](https://doi.org/10.1073/pnas.1208507109).
17. M. Jinek, K. Chylinski, I. Fonfara, M. Hauer, J. A. Doudna, E. Charpentier, A programmable dual-RNA-guided DNA endonuclease in adaptive bacterial immunity. *Science* **337**, 816-821 (2012). doi: [10.1126/science.1225829](https://doi.org/10.1126/science.1225829).
18. S. Y. Li, Q. X. Cheng, J. M. Wang, X. Y. Li, Z. L. Zhang, S. Gao, R. B. Cao, G. P. Zhao, J. Wang, CRISPR-Cas12a-assisted nucleic acid detection. *Cell discovery* **4**, 20 (2018). doi: [10.1038/s41421-018-0028-z](https://doi.org/10.1038/s41421-018-0028-z).
19. S. A. Bustin, T. Nolan, Pitfalls of quantitative real-time reverse-transcription polymerase chain reaction. *Journal of biomolecular techniques: JBT* **15**, 155-66 (2004).

20. M. Burns, H. Valdivia, Modelling the limit of detection in real-time quantitative PCR. *European Food Research and Technology* **226**, 1513-1524 (2007). doi: [10.1007/s00217-007-0683-z](https://doi.org/10.1007/s00217-007-0683-z).
21. A. Forootan, R. Sjoback, J. Bjorkman, B. Sjogreen, L. Linz, M. Kubista, Methods to determine limit of detection and limit of quantification in quantitative real-time PCR (qPCR). *Biomolecular detection and quantification* **12**, 1-6 (2017). doi: [10.1016/j.bdq.2017.04.001](https://doi.org/10.1016/j.bdq.2017.04.001).
22. W. Fu, Q. Chen, T. Wang, Letter to the Editor: Three cases of re-detectable positive SARS-CoV-2 RNA in recovered COVID-19 patients with antibodies. *Journal of medical virology*, (2020). doi: [10.1002/jmv.25968](https://doi.org/10.1002/jmv.25968)
23. B. Langmead, S. L. Salzberg, Fast gapped-read alignment with Bowtie 2. *Nature methods* **9**, 357-359 (2012). doi: [10.1038/nmeth.1923](https://doi.org/10.1038/nmeth.1923).
24. W. Z. Tieying Hou, Minling Yang, Wenjing Chen, Lili Ren, Jingwen Ai , Ji Wu, Yalong Liao, Xuejing Gou, Yongjun Li, Xiaorui Wang, Hang Su, Bing Gu, Jianwei Wang, Teng Xu, Development and Evaluation of A CRISPR-based Diagnostic For 2019-novel Coronavirus. *medRxiv* [preprint]. (2020). doi:[10.1101/2020.02.22.20025460](https://doi.org/10.1101/2020.02.22.20025460).

339



340

341 **Figure 1. Schematic description of SENA and its application as a confirmation diagnosis for**
342 **rRT-PCR diagnosis of COVID-19.** Generally, nucleic acids are extracted from the clinic
343 specimens such as pharyngeal swabs of the suspects of SARS-CoV-2 infection and then subject to
344 rRT-PCR analysis. The diagnostic reports are based on the Ct cut-off values guided by the supplier
345 of rRT-PCR kits. However, high Ct-value designated “grey zone” associated uncertain fuzzy
346 readouts are often encountered. Besides, some probably false-positive or false-negative cases may

be indicated by their atypical clinic symptoms or signs. For all these cases, the corresponding rRT-PCR products can be sent to another physically isolated room for SENA analysis and the ambiguity may be clarified by SENA with its positive and negative cut-off $mixFCratio$. The real-life data related to these scenarios revealed in this study are shown in the figure and details are illustrated in the text. RJ, JNCDC and SZII are the names of the hospitals and the number indicates the overall number of patients identified. While P140 was a patient in DF hospital, and two distinct samples from P140 were identified to be false-negative. For details, please ref to Supplementary **Table S3**.

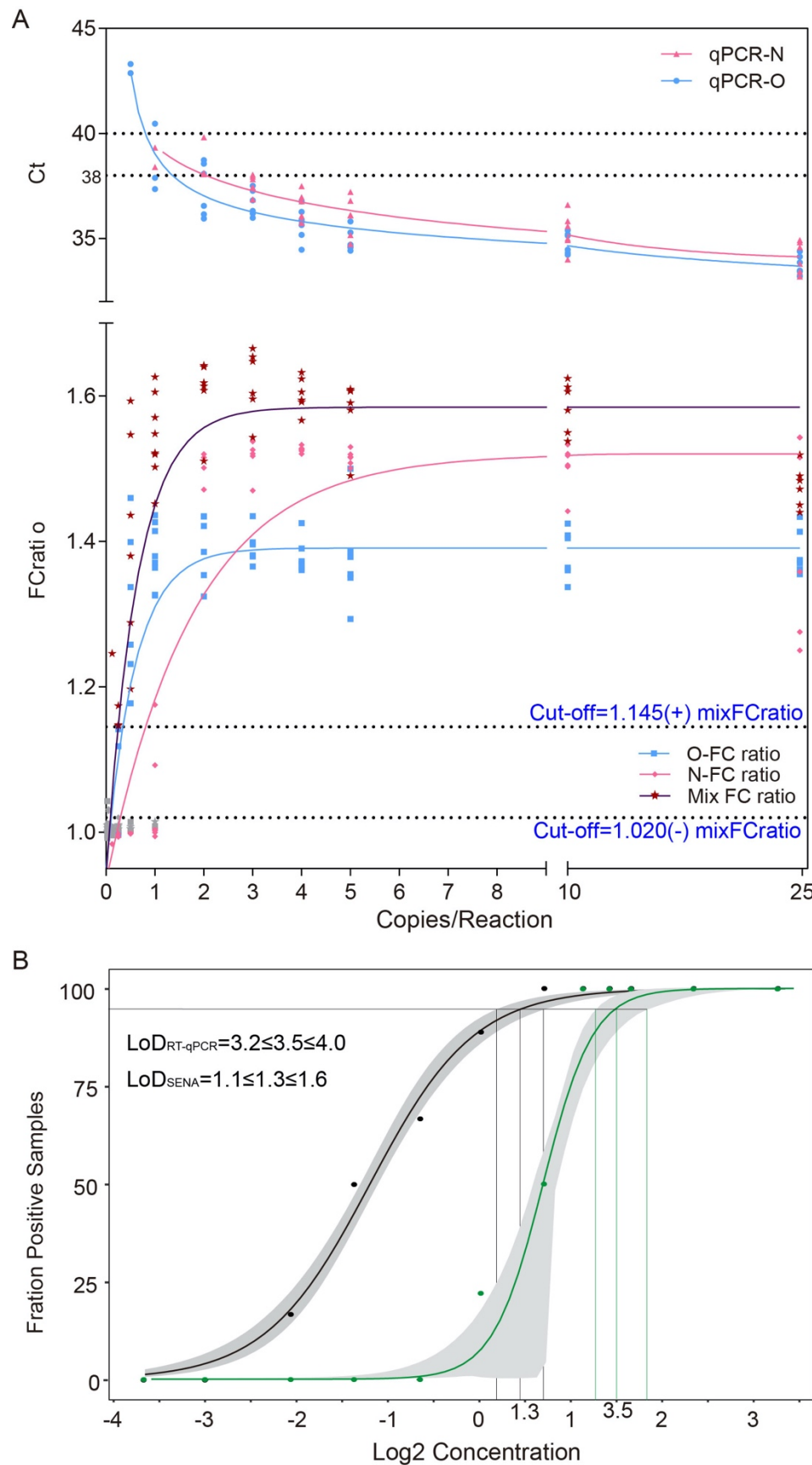


Figure 2. Determination of the cut-off values for SENA detection (A) and the LoD values with 95% CI for both rRT-PCR (O-Ct, green dots) and SENA (mix-FCratio, black dots) (B) based on the systematic titration assays. All the experimental and analytical details are described in the text. Notice that the SENA negative cut-off was set as mix-FCratio=1.020 in this figure on the basis of the titration assay of the standard RNA templates but was adjusted to 1.068 along with the increase of the clinic applications (**Figures 1 and 4, Supplementary Table S3**).

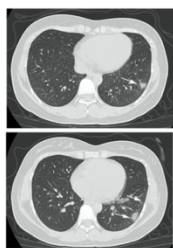
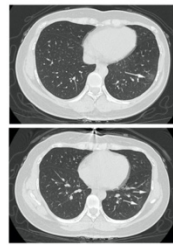
Date			Feb. 9			Feb. 11		Feb. 14		Feb. 15					
Hospitalization			Day1 (admitted)			Day3		Day6		Day7 (Discharged)					
Temperature(2P.M.) (°C)			36.7			36.9		36.9		36.7					
Lymphocyte(count, percentage) [§]			1.48*10 ⁹ /L, 36.3%			N/A		N/A		N/A					
Anti-SARS-CoV2 antibodies [#]	IgM		+			N/A		++		+					
	IgG		++			N/A		+++		+++					
Viral detection	Specimens*		a	b	c	a+b	c	b+c	e	b	c	a	d	e	f
	RT-qPCR (BJ)	Ct (O)	>40	>40	35.96	>40	>40	>40	>40	>40	>40	>40	>40	>40	>40
		Ct (N)	>40	>40	37.24	>40	>40	>40	>40	>40	>40	>40	>40	>40	>40
	SENA	mixFCratio	0.992	1.003	1.43	1.006	1.643	1.369	1.000	1.004	1.004	1.002	1.007	1.005	1.002
	NGS		N/A	N/A	+	N/A	+	+	N/A	N/A	-	N/A	N/A	N/A	N/A
Lung CT						N/A		N/A							

Figure 3. Schematic diagram of the hospitalization process of patient P140 (Shanghai DF Hospital). Detailed viral detection data are listed in **Table S3**. Other clinic data indicated that P140 is a COVID-19 patient with mild clinic symptoms.

[§]Reference range for Lymphocyte count: 1.1-3.2×10⁹/L; Reference range for the percentage of Lymphocyte: 20-50%.

[#]Label of the antibodies: +, weak; ++, medium; +++, strong.

^{*}Label of the specimens: a, pharyngeal swab; b, nasal (left) swab; c, nasal (right) swab; d, serum; e, plasma; f, fecal.

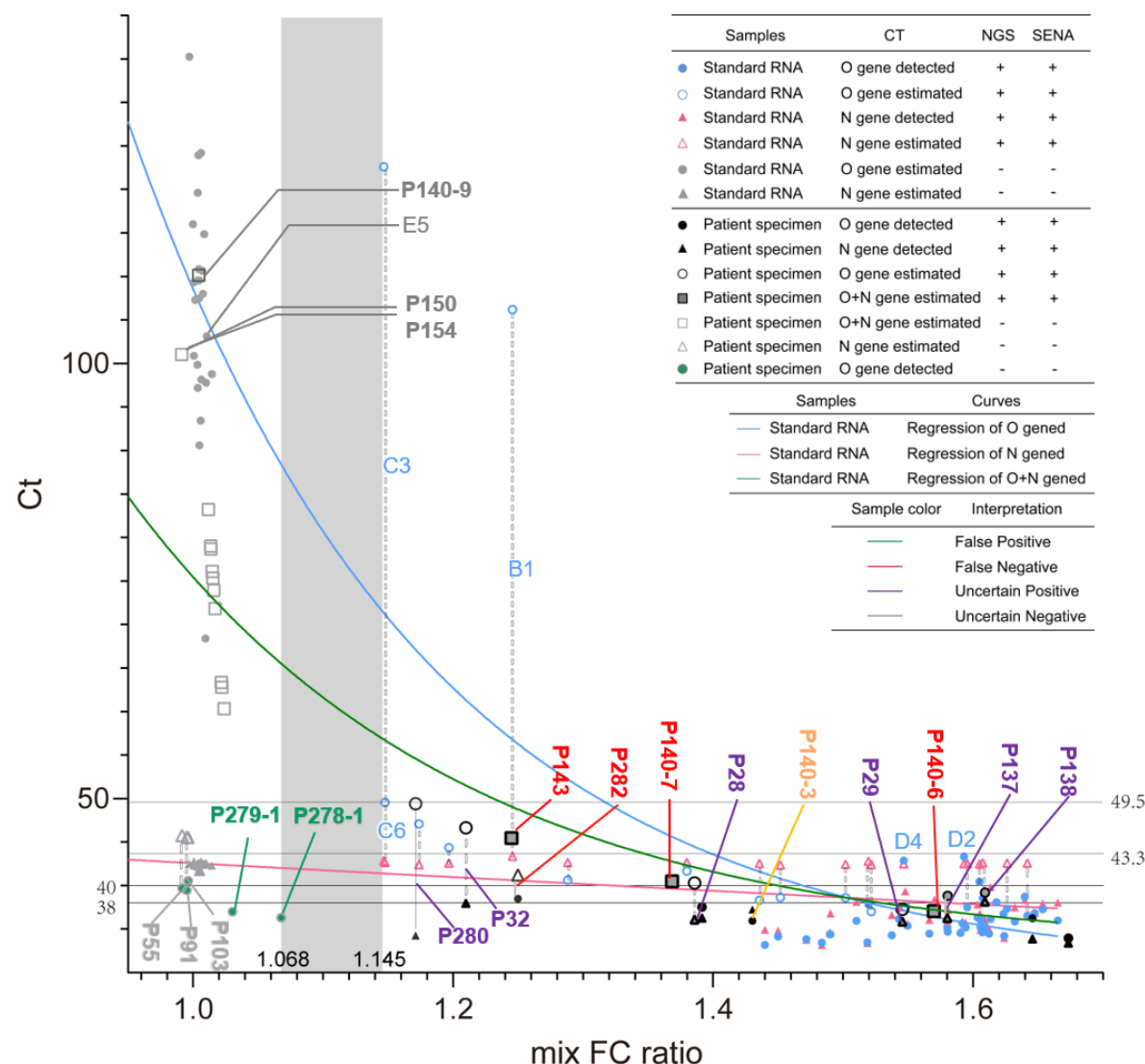


Figure 4. Apparent correlation plot of the rRT-PCR Ct values against the SENA mixFCratios in SARS-CoV-2 detection. All the data of the systematic titration experiment with low concentrations of standard RNA templates (Table S2A) and the data of clinic tests employing samples with ambiguous rRT-PCR readouts are used in this plot. In case the Ct values are too high to be detected by the rRT-PCR assay, i.e., Ct>40~45, depending on the scenarios, the mixFCratio-correlated “apparent Ct values” may be estimated via the template concentration-related regression functions (Materials and Methods 4.5); however, majority of the extremely high “apparent Ct values” in real negative samples are arbitrary and are adopted merely to simplify the presentation. The positive cut-off of the mix-SENA detection (mixFCratio=1.145) is defined by the C3 and C6 samples of the systematic titration experiment (Figure 2A), while the negative cut-off of the mix-SENA detection (mixFCratio=1.068) is defined by the P278-1 sample of the clinic tests (Table S3). This plot confirmed the cut-off Ct values of rRT-PCR test provided by the kit supplier (BJ, ref to all detectable Ct values shown as solid dots). Meanwhile, with the aid of mix-SENA, the sensitivity of rRT-PCR was increased up to the detected level of O-Ct=43.3 in samples of D2 and D4 and estimated level of O-Ct=49.5 in samples of C6 and P280. In addition, false positives were detected with O-Ct values as low as 39 (P278-1), which was also the key test to define the negative cut-off of mix-SENA.

Supplementary Materials for

A CRISPR-Cas12a-based specific enhancer for more sensitive detection of SARS-CoV-2 infection

Weiren Huang, Lei Yu, Donghua Wen, Dong Wei, Yangyang Sun, Huailong Zhao, Yu Ye, Wei Chen, Yongqiang Zhu, Lijun Wang, Li Wang, Wenjuan Wu, Qianqian Zhao, Yong Xu, Dayong Gu, Guohui Nie, Dongyi Zhu, Zhongliang Guo, Xiaoling Ma, Liman Niu, Yikun Huang, Yuchen Liu, Bo Peng, Renli Zhang, Xiuming Zhang, Dechang Li, Yang Liu, Guoliang Yang, Lanzheng Liu, Yunying Zhou, Yunshan Wang, Tieying Hou, Qiuping Gao, Wujiao Li, Shuo Chen, Xuejiao Hu, Mei Han, Huajun Zheng, Jianping Weng, Zhiming Cai, Xinxin Zhang, Fei Song*, Guoping Zhao*, Jin Wang*

*Correspondence to: F. S., lst121@outlook.com; G.Z., gpzhao@sibs.ac.cn; J.W., wangj01@hotmail.com.

This PDF file includes:

- Ethics statement
- Materials and Methods
- Figs. S1 to S5
- Tables S1 to S3

414
 415 **Ethics statement**
 416 The human pharyngeal swab samples were collected from residual samples that had been obtained for clinical
 417 respiratory virus detection. All procedures complied with the Measures for the Ethical Review of Biomedical Research
 418 Involving Human Subjects issued by the National Health and Family Planning Commission of The People's Republic
 419 of China. All protocols were approved by the Ethics Committees of Ruijin Hospital, Dongfang Hospital and Shenzhen
 420 Second People's Hospital. All procedures were performed in biosafety level 2 facilities.

421

422

Materials and Methods

1. RT-qPCR reactions.

Reactions were conducted in a 25- μ l reaction mixture following the instructions offered by the commercial suppliers of the reaction kits (ref to Supplementary **Table S1**). Usually, the reaction cycle parameters were set as reverse transcription at 50 °C for 10 min, denaturation at 95 °C for 5 min, then followed by 45 cycles of amplification, *i.e.*, 95 °C for 10 s and 55 °C for 40 s.

2. SENA reagents and detection.

2.1 Preparation of SENA reaction reagents

Candidate crRNA guide sequences with the “TTN” PAM sequences were designed as shown in Supplementary **Table S1**, and the crRNAs were prepared following the procedures previously described (11). Except the target DNA, the 2 \times SENA reagent comprises of 2 \times NEB buffer 3.1, 500 nM LbCas12a (Tolo Biotech.), 1 μ M synthesized crRNAs (for each specified target and thus varies according to the RT-qPCR kit supplier, **Table S1**), 1 μ M FQ-reporter, and 1 U/ μ l RNase inhibitor (TaKaRa).

2.2 SENA detection

To avoid the aerosol contamination of the MDx laboratory, after the RT-qPCR reaction, their products must be transferred to a physically isolated room to perform SENA detection. It is also important to choose proper SENA detection reagents corresponding to the RT-qPCR kits. To prepare a 20- μ l SENA reaction system, with corresponding positive and negative controls, 2- μ l PCR products and 8- μ l RNase-free H₂O were mixed with 10- μ l 2 \times SENA reagent, and the mixture was then measured on an appropriate fluorescence reader with FAM fluorescence collected following the programs: 48 °C 30 s per cycle, 20 cycles. Both the slope and the Fluorescence Change (FC) can be calculated at any time points as desired.

3. Next generation sequencing (NGS)

The RT-qPCR products were purified by AMPure XP beads (Beckman Coulter Life Sciences, US), and libraries were then constructed following the procedures of end repair, dA-tailing and adaptor ligation, with the StepWise DNA Lib Prep Kit for Illumina (ABclonal, China). After PCR amplification, samples were sequenced on Illumina Miniseq to produce 2 \times 150 bp paired-end reads. After adaptor trimming and quality trimming, the clean reads were mapped to the reference genome of SARS-CoV-2 (MN908947.3) using Bowtie2 (22).

4. Systematic titration and regression analyses

4.1 Systematic titration experimentation

4.1.1 The standard RNA templates

The SARS-CoV-2 RNA standards were purchased from Genewell (Shenzhen, China). According to the supplier's information, three plasmids containing the whole sequences of *N* and *E* genes, and partial sequence of the Orf1ab, *i.e.*, from 13237 to 13737 of the SARS-CoV-2 complete genome (MN908947.3), were transcribed *in vitro* individually. The RNA products were mixed with equal molar, aliquoted with addition of 1 μ g of human RNA per tube, and subject to lyophilization and subsequent quantification with digital PCR. This SARS-CoV-2 RNA standard dry powder containing 1808 copies of *O* gene, 1795 copies of *N* gene and 1160 copies of *E* gene was dissolved with 10 μ l RNase-free water to obtain the original stock solution (estimated 180.8 copies/ μ l of *O*, 179.5 copies/ μ l of *N* and 116 copies/ μ l of *E*).

4.1.2 The preparation of the serially diluted RNA templates

Pharyngeal swab samples were collected from 40 adult patients in Shenzhen Second Peoples' Hospital by the Clinic Diagnosis Laboratory and the nucleic acids of each sample were extracted with the pre-packaged nucleic acid extraction kit (Da'An Gene., Ltd., Guangzhou, China), according to the manufacturer's instructions, ended up with

55- μ l extracts per sample. After RT-qPCR assays employing 5 μ l of the extracts from each sample, all of the samples were shown to be SARS-CoV-2 negative. The remaining 50- μ l extracts of each sample were mixed together and 5 μ l of the mixture was once again analyzed by RT-qPCR and confirmed to be SARS-CoV-2 negative. Then, the mixed nucleic acid extract was used as the dilution buffer (totally about 2 ml) for serial dilution of the SARS-CoV-2 RNA standard stocks, generating desired concentrations (i.e., 5, 2, 1, 0.8, 0.6, 0.4, 0.2, 0.1, 0.05, 0.025, 0.01, 0.005 copies/ μ l), and 5 μ l of each of the diluted solutions were used as templates for RT-qPCR analysis, forming gradient template concentrations (i.e., 25, 10, 5, 4, 3, 2, 1, 0.5, 0.25, 0.125, 0.05, 0.025 copies/Rx).

4.1.3 Replica setting

We analyzed 9 replicas for each of the concentrations of 1 and 0.5 RNA template copies/Rx while 6 replicas for each of the rest concentrations (Supplementary **Figure S1**).

4.1.4 RT-qPCR reactions

RT-qPCR reaction kit was supplied by BJ (**Table S1**), who follows the primer sets recommended by Chinese CDC. Instead of the recommended 40 cycles of PCR amplification, we set 45 cycles as routine aiming at recording the maximum exact Ct values if possible.

4.1.5 SENA detection

Every amplicon of the RT-qPCR reactions was subjected to SENA detection. Specially, for this experimentation, three sets of SENA reagents were individually used, O-SENA contains the crRNA targeting the *O* sequence, N-SENA contains the *N*-targeting crRNA, and the mix-SENA contains crRNAs for both sequences.

4.2 Choice of *FCratio* as the standard readout for SENA detection and mix-SENA as the standard reagent for clinic application

Three readout parameters were compared as shown in **Figure S1** (original data in **Table S2**). The slope (increase of fluorescence/min) represents the reaction rate of Cas12a *trans*-cleavage activity, but in this experiment, it represents neither the initial rate of the enzyme under limited substrate condition nor the pure first-order reaction rate varies according to the substrate concentration, particularly, demonstrated in cases of high template concentration, in which, the slope goes down along with the increase of the template concentration. In addition, when the substrate concentration is low, the slope of SENA is hard to be distinguished from that of the negative control, ending with ambiguous cut-offs. The FC (the fold of change of fluorescence between that of the sample over that of the negative control at certain time point, usually 5-30 min) does show clear differences between the positive amplicons from that of negative control, and it also shows certain quantitation character particularly at the low concentration templates cases. Because of these properties, FC has been a parameter used by a few users of CRISPR-Dx (24). However, it seems that the absolute value of the FC usually varies along the reaction time and sometimes it is influenced by the change of the fluorescence signal of the negative control. Besides, it is difficult to determine the “best choice” of the FC recorded at certain time points, which may cause confusing in clinic applications. It is clear, we need a stable readout which reflects the dynamic process and the quantitative correlation of SENA reaction with the low concentration of the templates on one hand and should be robust and accurate for clinical diagnosis on the other hand. We defined *FCratio*, which is the ratio between FC's of SENA detection at 10 min versus 5 min after the beginning of the fluorescence reading. It not only measures the fluorescence change of SENA against the negative control background so that the quantity of the amplicons, particularly at the low concentration range may be represented, but also normalizes the slope of the fluorescence change of SENA to eliminate the complex background differences. As shown in **Figure S2**, *FCratio* significantly amplified the positive signals and represents the quantitation of the amplicons at low template concentrations to certain extent.

As shown in **Figure S1**, the capacity of the three SENA reactions are compared. It is obvious that N-SENA is the least sensitive one, while although O-SENA seems much more sensitive than that of N-SENA and largely comparable to that of mix-SENA, its signal at the very low template concentration range seems uncertain in some cases. Therefore, for clinic application, mix-SENA is the choice.

4.3 Quality analyses of the RT-qPCR titration data

The quality of the Ct values vs the concentration of the standard templates for RT-qPCR of the systematic titration experiment were analyzed both empirically and statistically. Firstly, as shown in **Table S2** and **Figure S1**, the amplification efficiencies of the two genes represented by the valuable Ct readouts were different. The apparently lower sensitivity of the *N* gene amplification is in contrast with the clinic experiences and might due to the difference

in the property of the templates used in different experiments (laboratory standard RNA template vs clinical real viral template). Secondly, although linear regression can be readily made between the Ct-values and the log10 (conc) (Figure S3A) as that of the previously published tests, the quality of the regression as judged by the R^2 s (Figure S3A) and the residues (Figure S3B) are clearly suboptimal likely due to the limited number of replicas in the experimentation. On the other hand, this titration was designed with taking at least the two most fundamental limitation factors about the sensitivity of COVID-19 RT-qPCR diagnosis into consideration, *i.e.*, the sampling ambiguity and the influence of the biological/chemical contaminants from the clinic samples. Therefore, the data will be used for determination of the LoD for RT-qPCR and SENA (Materials and Methods 4.4 and Figure S2), and the regression function will be used to estimate the “apparent Ct” values of the samples with Ct-values greater than 45 (no amplification signal) but their SENA detection is positive (Materials and Methods 4.5 and Figure S4).

4.4 Determination of limit of detection (LoD) for RT-qPCR and SENA

The LoD values for RT-qPCR (N-Ct and O-Ct) and SENA (N-FCratio, O-FCratio and mix-FCratio) were estimated based on the systematic titration employing standard RNA templates (Figure S1 and Table S2). The fractions of positive replicates versus the number of target molecules (copies) per reaction for N and O gene of COVID-19 were plotted and used the sigmoidal function (1) to fit the data via R (software version 3.5.0). The 95% confidence intervals were derived by bootstrapping the model residues and were visualized by R (software version 3.5.0) with built-in ggplot2 library (21).

4.5 Regression of RT-qPCR Ct-values and the SENA FCratio versus the concentration of the templates employing the data from the systematic titration

$$y_i = \frac{1}{1 + e^{-\alpha - \beta \log(c_i)}} \quad (1)$$

4.5.1 Regression of RT-qPCR Ct-values with the concentration of the templates (copies/Rx)

Since PCR product increased exponentially with the initial concentration of the sample (x), and the Ct value of RT-qPCR parameter (y) was inversely correlated with the initial concentration, especially in the range of low copy number (low template concentration) samples, the power function equation ($a < 1$) should be suitable for the data fitting. However, some of the experimental groups included very low initial sample concentrations (< 1 copy/Rx), those amplification efficiencies should be different (particularly affected by sampling ambiguity) from that of the groups with high initial template concentration. Therefore, the power function formula with four parameters ($Y = aX^n + bX^m$) was used to match all the experimental group data to obtain a more accurate data model (Functions 1, Figure S4).

4.5.2 Regression of SENA FCratio with the concentration of the templates (copies/Rx)

The exponential function (first order association kinetics of the interaction between a substrate and an enzyme, $Y = a + b(1 - e^{-cX})$) is used to fit the data of FCratio against the concentration of the templates. At low concentration (especially when the concentration is less than 2 copies/Rx), the FCratio is positively correlated with the template concentrations. However, when the template concentration reaches to 2 copies/Rx and more, the FCratio does not increase accordingly and the curve tend to be flatted out. In addition, as FCratio have been already normalized by the fluorescence signal of the negative background, it is stable and, in this case, we give the parameter Y_0 being set as a constant value between 0.9 to 1 (Functions 2, Figure S5).

4.5.3 Regression of RT-qPCR Ct-values with the SENA mix-FCratio values

In practice, quite significant portions of the clinic positive samples detected by mix-SENA with their FCratio readings higher than the positive cut-off, but with a negative PCR Ct value ($> 40-45$, depending on the scenario). Under certain circumstances, people may be interested to learn the copy number of the templates for the corresponding RT-qPCR assays or even the “probable” Ct values of these assays. With the aid of the above-mentioned two regression functions (1 in Figure S4 and 2 in Figure S5), these data could be estimated. One may firstly substitute the Y in Function 2 by the measured FCratio value and the corresponding X can be calculated representing the “estimated concentration of the template). Then this X value can be used to estimate the corresponding “estimated Ct-value” as the Y of Function 1. We estimated all the ambiguous Ct-values of the positive amplicons and plotted them against their corresponding mix-FCratio (Figure 4). All the real and estimated Ct values for both N and O genes are plotted against the corresponding FCratio values of mix-SENA as X axis. An exponential decay function (with $X_0 = 1$; When $X \leq X_0$,

Ct=∞; otherwise, one phase decay) fits well to all the data ($R^2=0.9238$) and is used for analyzing the clinic data and adjust the cut-off values accordingly (**Figure 4**).

5. Detection of antibodies

The detection of anti-SARS-CoV2 antibodies was executed by the point-of-care microfluidic platform integrating a home-made fluorescence detection analyzer (Suxin, Shanghai, China). A total of 10-μl plasma was added into the loading chamber of microchip followed by the addition of 70-μl sample dilution buffer. After incubation for 15 min at room temperature, the microchips were loaded onto the fluorescence detection analyzer, and fluorescence signal was detected from the analyzer, following the manufacturer's instruction.

Supplementary Figures

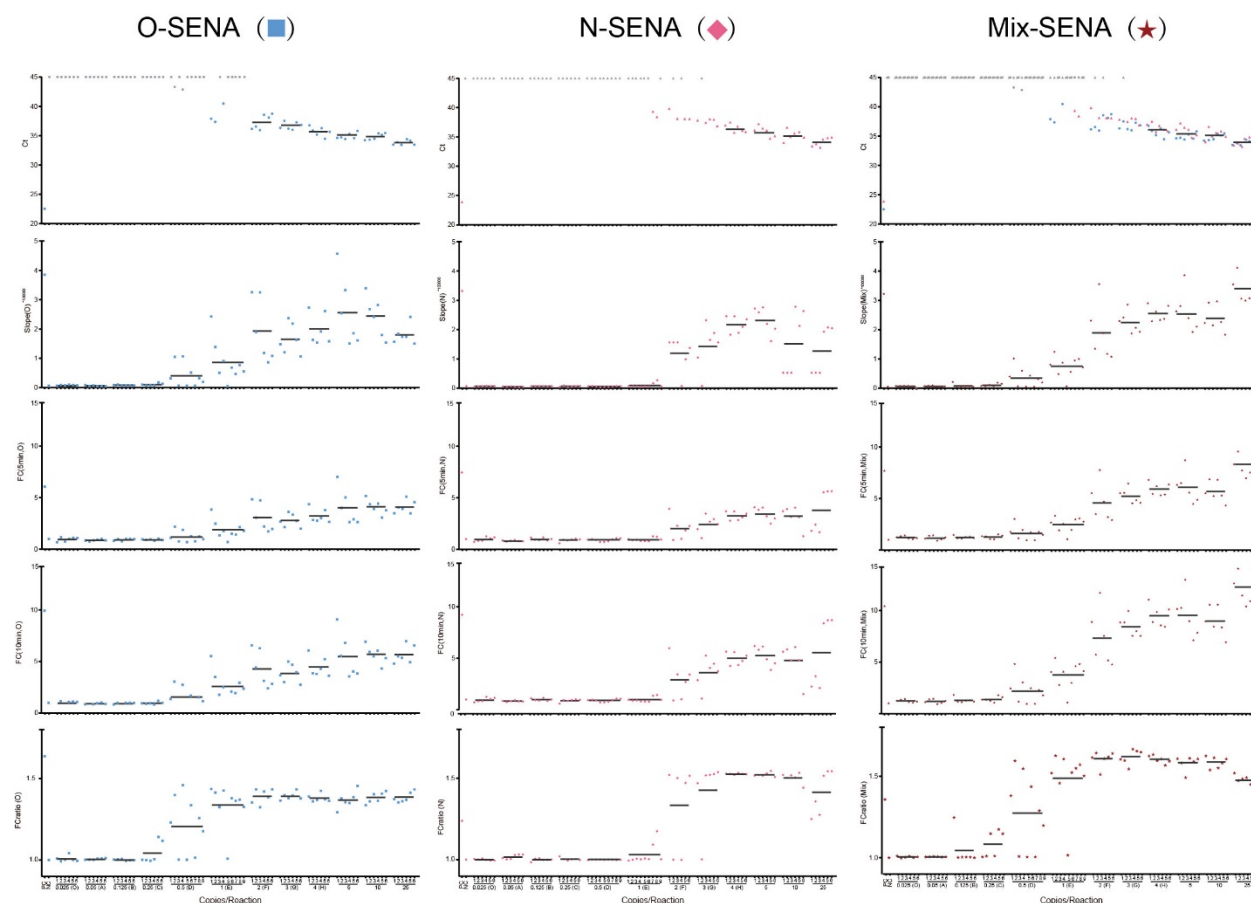


Fig. S1. Systematic titration of serially diluted SARS-CoV-2 standard RNA templates detected by RT-qPCR followed by SENA. The design of this experiment is illustrated in detail in *Materials and Methods 4*. All the resulted readouts are listed in Table S2 and are plotted in this figure for individual tests being numbered with each of the concentration of the templates used as marked in the bottom X-axis. The very top horizontal row of the panel matrix is the test of RT-qPCR with Ct values detected via fluorescence of FAM (● for O gene), VIC (▲ for N gene) and both, respectively. In case $Ct \geq 45$, i.e., no fluorescence signal of PCR amplification could be detected, the corresponding symbols were shown in grey (● or ▲). The vertical lists from the second row of the panel matrix represent the SENA reagent used for the detection: O-SENA (■), N-SENA (◆) and mix-SENA (★). The parameters of SENA detection are shown from the second top row to the bottom row as slope-5min, FC-5min, FC-10min and FCratio-10min/5min (abbreviated as *FCratio*), respectively and are all marked on their corresponding Y-axis. The RT-qPCR amplicons were all subject for NGS for verification (Table S2).

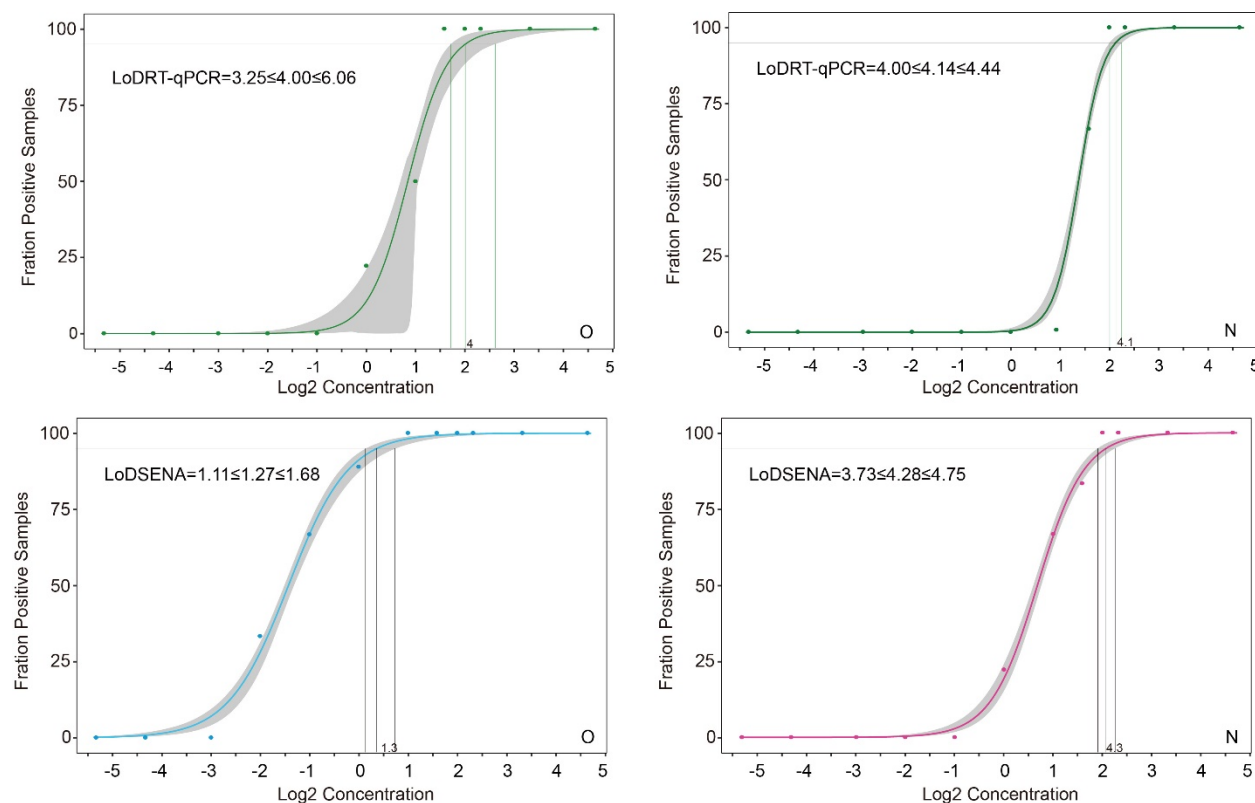


Fig. S2. Determination of the LoD values with 95% CI for both RT-qPCR (O-Ct and N-Ct, both green dots) and SENA (N-FCratio, pink dots; and O-FCratio, blue dots) based on the systematic titration (Materials and Methods 4.4). All the experimental and analytical details are described in the text.

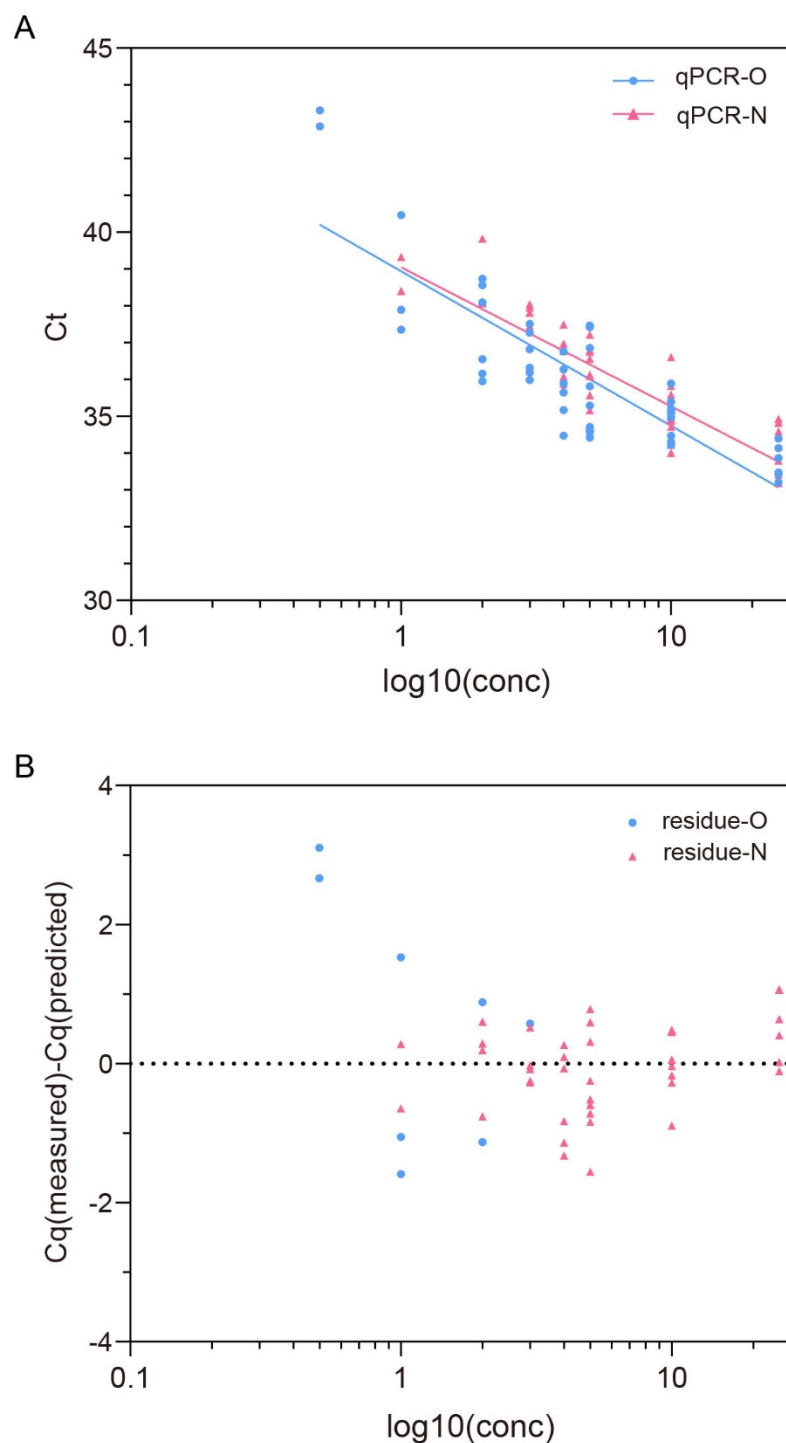


Fig. S3. Linear regression (A) of the Ct values (● for O gene and ▲ for N gene) corresponding to the RT-qPCR titration experiment. The regression function for Ct (O) is: $Y=38.94-4.198*\log(x)$ ($R^2=0.7126$) and the regression function for Ct (N) is: $Y=39.05-3.776*\log(x)$ ($R^2=0.7662$), Panel B is the residue plot for these two regressions.

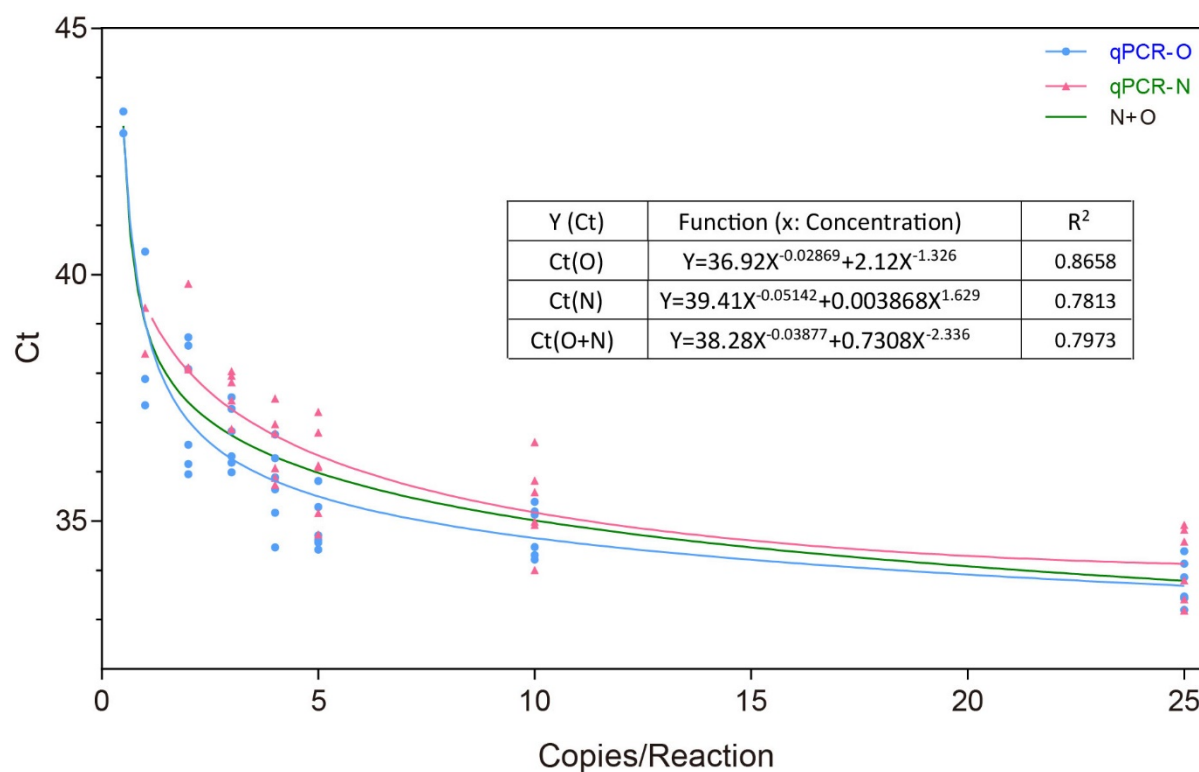


Fig. S4. Regression of RT-qPCR Ct-values with the concentration of the templates (copies/Rx). The data is from Table S2. The regression functions for Ct-values of O gene (—), N gene (—) and both (—) (Functions 1) are illustrated as a table inside of the panel.

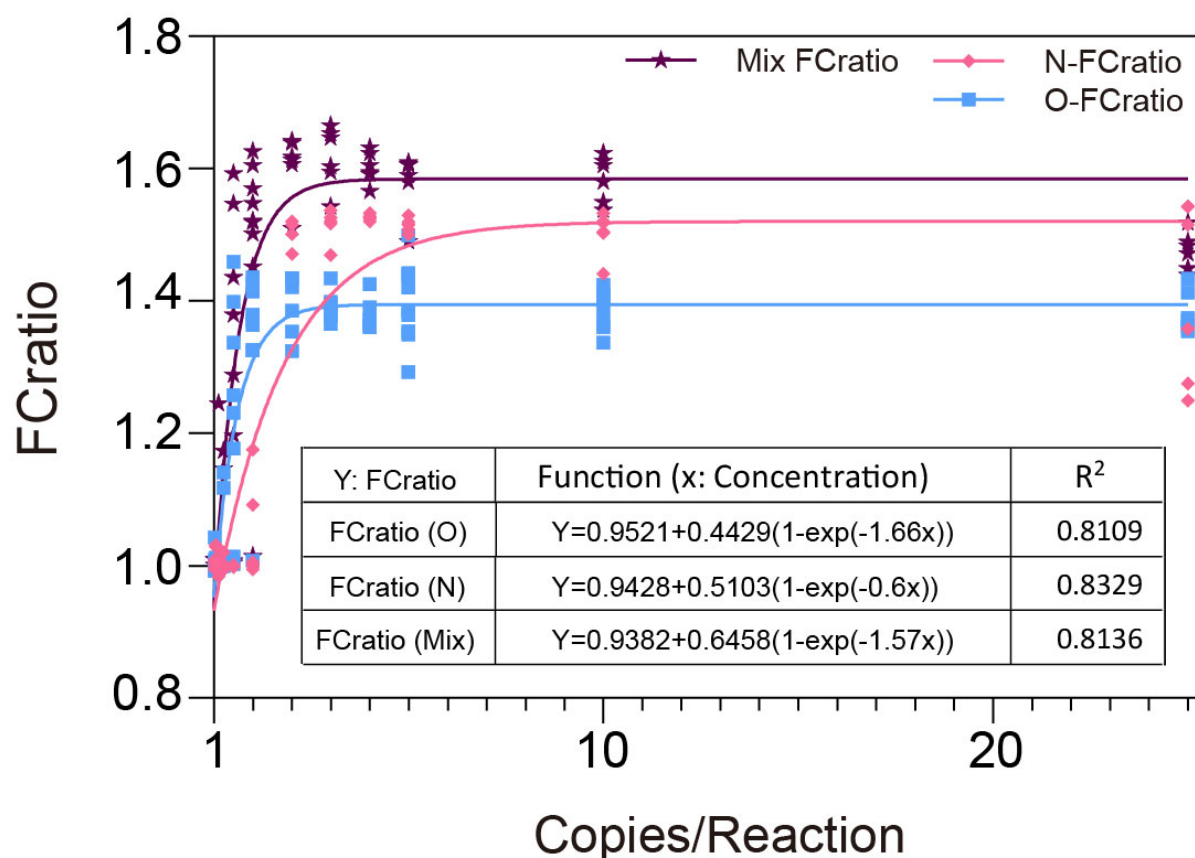


Fig. S5. Regression of SENA *FCratio* with the concentration of the templates (copies/Rx). The data is from Table S2. The regression functions for *FCratios* of O-SENA (—), N-SENA (—) and mix-SENA (—) (Functions 2) are illustrated as a table inside of the panel.

Table S1. Oligo nucleotide sequences of crRNA for SENA assay in this study

crRNA	Oligo nucleotide (5'-3') ^a	Target genes	Standards ^b
crRNA_ZJ_O4	<i>TGTCTGATGTTGGTGATAGTGCGATCTACAAG</i> AGTAGAAATTCCTATAGTGAGTCGTATTA	<i>O</i>	WHO (ZJ)
crRNA5.3.1	<i>AGTGTAAGTACAGCAAGATACCATCTACAAG</i> AGTAGAAATTCCTATAGTGAGTCGTATTA	<i>E</i>	WHO (ZJ)
FcrRNA3.7.1	<i>GGAGTTGATCACAACTACAGCCAATCTACAAG</i> AGTAGAAATTCCTATAGTGAGTCGTATTA	<i>O</i>	Chinese CDC (BJ)
FcrRNA6.7.1	<i>CAATCTGTCAAGCAGCAGCAAGATCTACAAG</i> AGTAGAAATTCCTATAGTGAGTCGTATTA	<i>N</i>	Chinese CDC (BJ)
crRNA_HD_O1	<i>ACAGTTTGTGACTATCATCATCTACAAGA</i> GTAGAAATTCCTATAGTGAGTCGTATTA	<i>O</i>	(HD)

Note:

^aThe nucleic acid sequences complementary to the guide sequences are shown in italic and the bolded sequences were complementary to the direct repeats (DR) of LbCas12a crRNA. The underlined sequence was complementary to the T7 promoter, and thus, able to be aligned with the T7 promoter to initiate the T7 RNA polymerase catalyzed *in vitro* transcription to synthesize the designed crRNA.

^bcrRNAs prepared with the oligo nucleotides listed in this table specifically target the RT-qPCR amplified gene fragments of *O*, *E* or *N* in SARS-CoV-2, designed by the suppliers (labeled in the parenthesis) of individual commercial kits based on the standards of WHO, Chinese CDC or itself.

Table S2-A Original data of the titration experiment (Low template conc).

Tests		Ct		N-SENA				O-SENA				mix-SENA				NGS reads	
Conc	Replica	O	N	Slope (x100000)	FC 5min	FC 10min	Fcratio	Slope (x100000)	FC 5min	FC 10min	Fcratio	Slope (x100000)	FC 5min	FC 10min	Fcratio	Total	Matched
0.025 Copies/Rx	O1	UD	UD	0.068	1.138	1.120	0.984	0.086	0.835	0.838	1.004	0.215	1.465	1.825	1.246	/	/
	O2	UD	UD	0.073	0.933	0.939	1.006	0.100	0.981	0.987	1.007	0.059	1.153	1.154	1.001	/	/
	O3	UD	UD	0.072	0.884	0.891	1.008	0.067	0.772	0.778	1.007	0.056	1.118	1.121	1.003	/	/
	O4	UD	UD	0.069	1.160	1.159	0.999	0.072	1.004	1.000	0.996	0.066	1.253	1.259	1.004	/	/
	O5	UD	UD	0.058	0.862	0.862	1.000	0.067	1.005	1.003	0.997	0.072	1.289	1.294	1.004	/	/
	O6	UD	UD	0.071	0.998	1.000	1.002	0.065	0.980	0.979	0.999	0.056	1.168	1.168	1.000	/	/
0.05 Copies/Rx	A1	UD	UD	0.043	0.589	0.601	1.020	0.098	0.943	0.944	1.001	0.080	1.344	1.350	1.005	/	/
	A2	UD	UD	0.092	0.941	0.943	1.002	0.070	0.899	0.898	0.999	0.072	1.331	1.343	1.009	/	/
	A3	UD	UD	0.041	0.870	0.865	0.995	0.090	0.943	0.940	0.996	0.110	1.079	1.237	1.147	/	/
	A4	UD	UD	0.058	0.954	0.956	1.002	0.070	0.828	0.833	1.005	0.067	1.048	1.059	1.011	/	/
	A5	UD	UD	0.065	1.022	1.026	1.004	0.177	1.039	1.186	1.142	0.196	1.521	1.785	1.174	/	/
	A6	UD	UD	0.075	0.968	0.966	0.998	0.132	0.890	0.995	1.118	0.155	1.386	1.591	1.148	/	/
0.125 Copies/Rx	B1	UD	UD	0.068	1.138	1.120	0.984	0.086	0.835	0.838	1.004	0.215	1.465	1.825	1.246	243811	535
	B2	UD	UD	0.073	0.933	0.939	1.006	0.100	0.981	0.987	1.007	0.059	1.153	1.154	1.001	291449	0
	B3	UD	UD	0.072	0.884	0.891	1.008	0.067	0.772	0.778	1.007	0.056	1.118	1.121	1.003	359220	0
	B4	UD	UD	0.069	1.160	1.159	0.999	0.072	1.004	1.000	0.996	0.066	1.253	1.259	1.004	268425	0
	B5	UD	UD	0.058	0.862	0.862	1.000	0.067	1.005	1.003	0.997	0.072	1.289	1.294	1.004	271915	0
	B6	UD	UD	0.071	0.998	1.000	1.002	0.065	0.980	0.979	0.999	0.056	1.168	1.168	1.000	347723	0
0.25 Copies/Rx	C1	UD	UD	0.043	0.589	0.601	1.020	0.098	0.943	0.944	1.001	0.080	1.344	1.350	1.005	280487	0
	C2	UD	UD	0.092	0.941	0.943	1.002	0.070	0.899	0.898	0.999	0.072	1.331	1.343	1.009	327392	0
	C3	UD	UD	0.041	0.870	0.865	0.995	0.090	0.943	0.940	0.996	0.110	1.079	1.237	1.147	370753	570
	C4	UD	UD	0.058	0.954	0.956	1.002	0.070	0.828	0.833	1.005	0.067	1.048	1.059	1.011	313561	2
	C5	UD	UD	0.065	1.022	1.026	1.004	0.177	1.039	1.186	1.142	0.196	1.521	1.785	1.174	313109	59
	C6	UD	UD	0.075	0.968	0.966	0.998	0.132	0.890	0.995	1.118	0.155	1.386	1.591	1.148	332895	47
0.5 Copies/Rx	D1	UD	UD	0.068	0.931	0.929	0.998	0.315	1.108	1.365	1.231	0.401	1.767	2.438	1.380	360678	73
	D2	43.31	UD	0.075	0.980	0.982	1.001	1.052	2.184	3.055	1.399	1.016	3.015	4.803	1.593	394441	54
	D3	UD	UD	0.049	0.903	0.903	1.001	0.061	0.765	0.767	1.003	0.064	1.153	1.162	1.008	289948	0

1 Copies/Rx	D4	42.87	UD	0.041	0.713	0.714	1.001	1.069	1.878	2.741	1.460	0.595	1.951	3.017	1.547	313613	115
	D5	UD	UD	0.047	0.723	0.723	1.000	0.059	0.687	0.688	1.002	0.056	0.938	0.943	1.005	328563	0
	D6	UD	UD	0.051	0.787	0.788	1.001	0.511	1.259	1.683	1.337	0.436	1.719	2.468	1.436	372990	64
	D7	UD	UD	0.057	0.965	0.965	1.000	0.058	0.776	0.787	1.014	0.055	0.944	0.948	1.005	333039	0
	D8	UD	UD	0.070	1.085	1.083	0.998	0.317	1.230	1.548	1.258	0.314	1.765	2.274	1.288	360707	153
	D9	UD	UD	0.068	1.068	1.068	1.000	0.190	0.984	1.159	1.177	0.201	1.477	1.768	1.197	212757	113
	E1	37.89	UD	0.076	0.979	0.974	0.994	2.426	3.844	5.520	1.436	0.803	2.659	4.041	1.520	269723	217
	E2	37.35	UD	0.064	0.884	0.884	1.000	1.386	2.478	3.505	1.414	1.245	3.318	5.395	1.626	457749	219
	E3	UD	UD	0.066	0.906	0.911	1.005	0.502	1.338	1.773	1.325	0.489	1.906	2.777	1.458	369267	69
	E4	40.47	UD	0.053	0.822	0.824	1.002	0.907	1.759	2.509	1.426	0.875	2.524	4.051	1.605	238968	294
2 Copies/Rx	E5	UD	UD	0.064	0.799	0.805	1.007	0.049	0.704	0.710	1.008	0.069	1.055	1.071	1.015	317126	4
	E6	UD	UD	0.057	0.789	0.791	1.003	0.682	1.506	2.077	1.379	0.561	1.962	2.985	1.522	252167	172
	E7	UD	39.33	0.171	1.255	1.370	1.092	0.466	1.425	1.943	1.364	0.948	2.977	4.608	1.548	94314	649
	E8	UD	38.40	0.272	1.218	1.431	1.175	0.772	2.145	2.940	1.371	1.001	3.061	4.807	1.570	345634	1183
	E9	UD	UD	0.063	0.958	0.960	1.003	0.551	1.784	2.366	1.326	0.721	2.735	4.108	1.502	296593	383
	F1	36.16	39.82	1.566	3.926	5.968	1.520	3.253	4.850	6.565	1.354	2.309	5.504	8.881	1.614	59563	173
	F2	36.55	UD	1.566	0.906	0.906	1.000	1.889	3.074	4.408	1.434	1.353	3.482	5.716	1.642	3736	116
	F3	35.95	38.12	1.566	2.287	3.434	1.501	3.251	4.742	6.279	1.324	3.554	7.748	11.703	1.510	334475	0
	F4	38.56	UD	0.078	1.027	1.026	0.998	1.182	2.199	3.125	1.421	1.885	4.694	7.546	1.607	257994	0
	F5	38.09	38.08	0.989	1.842	2.710	1.471	0.864	1.729	2.396	1.386	1.175	3.195	5.169	1.618	243367	418
3 Copies/Rx	F6	38.73	38.07	1.375	2.261	3.427	1.515	1.079	1.972	2.828	1.434	1.076	2.910	4.772	1.640	253600	148
	G1	36.32	37.82	1.046	1.955	2.874	1.470	1.476	2.678	3.657	1.365	2.295	5.505	8.828	1.604	/	/
	G2	37.51	UD	0.077	1.089	1.091	1.002	1.204	2.146	3.001	1.399	2.416	5.537	8.834	1.596	/	/
	G3	36.19	37.45	2.320	3.467	5.261	1.517	2.370	3.623	5.003	1.381	2.856	6.450	9.951	1.543	/	/
	G4	35.99	38.04	1.649	2.674	4.066	1.521	2.182	3.353	4.680	1.396	1.869	4.530	7.544	1.665	/	/
	G5	37.28	37.95	1.884	2.929	4.469	1.526	1.632	2.766	3.968	1.434	2.061	4.830	7.988	1.654	/	/
	G6	36.82	36.87	1.566	2.434	3.742	1.537	1.068	1.993	2.749	1.379	1.933	4.580	7.544	1.647	/	/
	H1	36.76	36.97	2.458	3.687	5.634	1.528	2.730	4.359	6.059	1.390	2.904	6.800	11.041	1.624	/	/
	H2	35.89	37.49	1.826	2.780	4.245	1.527	1.629	2.830	3.850	1.361	2.291	5.442	8.883	1.632	/	/
	H3	35.17	35.74	2.455	3.681	5.597	1.520	1.538	2.774	3.799	1.369	2.616	6.185	9.861	1.594	/	/
4 Copies/Rx	H4	36.28	36.78	1.893	2.832	4.340	1.533	1.916	3.021	4.305	1.425	2.332	5.328	8.553	1.605	/	/
	H5	34.47	36.08	2.095	3.103	4.735	1.526	2.614	3.803	5.219	1.372	2.370	5.383	8.432	1.567	/	/

5 Copies/Rx	H6	35.65	35.88	2.349	3.443	5.248	1.524	1.580	2.665	3.633	1.363	2.817	6.343	10.098	1.592	/	/
	I1	34.61	36.13	2.720	4.079	6.185	1.516	4.567	7.015	9.071	1.293	2.631	6.312	10.145	1.607	/	/
	I2	34.71	37.22	2.589	3.831	5.823	1.520	2.537	4.017	5.538	1.379	2.805	6.481	10.243	1.580	/	/
	I3	34.42	36.46	2.759	4.047	6.133	1.515	3.327	5.023	6.806	1.355	3.858	8.710	12.980	1.490	/	/
	I4	35.29	36.09	2.196	3.205	4.903	1.530	1.503	2.635	3.556	1.350	2.395	5.572	8.967	1.609	/	/
	I5	34.57	34.73	1.607	2.499	3.860	1.545	1.852	2.908	4.030	1.386	1.922	4.474	7.115	1.590	/	/
	I6	35.81	35.16	2.029	2.992	4.512	1.508	1.610	2.629	3.825	1.455	2.106	4.870	7.825	1.607	/	/

Note: UD, undetected. /, PCR product was not analyzed by NGS.

Table S2-B Original data of the titration experiment (High template conc).

Tests		Ct		N-SENA				O-SENA				mix-SENA				NGS reads	
Conc	Replica	O	N	Slope (x100000)	FC 5min	FC 10min	Fcratio	Slope (x100000)	FC 5min	FC 10min	Fcratio	Slope (x100000)	FC 5min	FC 10min	Fcratio	Total	Matched
10 Copies/Rx	J1	34.23	34.01	0.528	3.700	5.625	1.520	3.394	5.168	6.910	1.337	2.232	5.499	8.931	1.624	/	/
	J2	34.31	36.61	0.528	3.898	5.857	1.503	2.679	4.355	5.923	1.360	2.921	6.863	10.553	1.538	/	/
	J3	34.47	34.99	0.528	3.163	4.802	1.518	2.412	3.913	5.495	1.404	2.146	5.230	8.432	1.612	/	/
	J4	35.39	35.59	2.785	4.042	6.083	1.505	2.817	4.434	6.047	1.364	2.966	6.814	10.559	1.550	/	/
	J5	35.14	35.82	2.130	3.131	4.801	1.533	1.794	3.069	4.321	1.408	2.258	5.290	8.360	1.580	/	/
	J6	35.45	34.92	2.637	1.273	1.526	1.442	1.539	3.772	5.327	1.424	1.834	4.311	6.923	1.606	/	/
25 Copies/Rx	H1	33.47	33.42	0.528	1.798	2.247	1.250	1.560	3.491	4.798	1.374	3.551	8.312	12.625	1.519	/	/
	H2	33.86	33.80	0.528	2.398	3.256	1.358	1.842	4.055	5.493	1.355	4.112	9.547	14.051	1.472	/	/
	H3	33.43	33.19	0.528	1.655	2.111	1.276	1.738	3.922	5.339	1.361	3.062	7.712	11.442	1.484	/	/
	H4	34.39	34.59	1.930	5.532	8.381	1.515	1.738	5.083	6.964	1.370	2.991	6.980	10.400	1.490	/	/
	H5	34.14	34.82	2.073	5.624	8.676	1.543	2.412	3.485	4.925	1.413	3.071	7.517	10.900	1.450	/	/
	H6	33.45	34.92	2.047	5.634	8.693	1.543	1.502	4.567	6.548	1.434	3.605	9.792	14.100	1.440	/	/

Note: /, PCR product was not analyzed by NGS.

Table S3. Comparison of SARS-CoV-2 measurement on clinical specimens by RT-qPCR and SENA

Patient No.	Specimens	Clinical features		qPCR				SENA		NGS	Final outcome	Sample origin
		Symptoms	Diagnosis	Ct Value (E)	Ct Value (O)	Ct Value (N)	Interpretation	FCratio Value	Interpretation			
P001	Oropharyngeal swab	Fever, cough	COVID-19 suspected	N/A	29.55	29.47	+	1.584	+	/	Consistent Positive	SZII
P002	Oropharyngeal swab	Fever, cough	COVID-19 suspected	N/A	26.91	27.04	+	1.640	+	/	Consistent Positive	SZII
P003	Oropharyngeal swab	Fever, cough	COVID-19 suspected	N/A	33.77	33.88	+	1.570	+	/	Consistent Positive	SZII
P004	Oropharyngeal swab	Fever, cough	COVID-19 suspected	N/A	33.47	33.46	+	1.587	+	/	Consistent Positive	SZII
P005	Oropharyngeal swab	Fever, cough	COVID-19 suspected	N/A	33.83	34.24	+	1.553	+	/	Consistent Positive	SZII
P006	Oropharyngeal swab	Fever, cough	COVID-19 suspected	N/A	32.6	32.4	+	1.589	+	/	Consistent Positive	SZII
P007	Oropharyngeal swab	Fever, cough	COVID-19 suspected	N/A	33.72	34.47	+	1.550	+	/	Consistent Positive	SZII
P008	Oropharyngeal swab	Fever, cough	COVID-19 suspected	N/A	30.13	29.73	+	1.578	+	/	Consistent Positive	SZII
P009	Oropharyngeal swab	Fever, cough	COVID-19 suspected	N/A	34.75	34.81	+	1.535	+	/	Consistent Positive	SZII
P010	Oropharyngeal swab	Fever, cough	COVID-19 suspected	N/A	30.54	30.72	+	1.617	+	/	Consistent Positive	SZII
P011	Oropharyngeal swab	Asymptomatic	Close contacts	N/A	>40	>40	-	1.003	-	/	Consistent Negative	SZII
P012	Oropharyngeal swab	Asymptomatic	Close contacts	N/A	>40	>40	-	0.995	-	/	Consistent Negative	SZII
P013	Oropharyngeal swab	Asymptomatic	Close contacts	N/A	>40	>40	-	0.998	-	/	Consistent Negative	SZII
P014	Oropharyngeal swab	Asymptomatic	Close contacts	N/A	>40	>40	-	1.000	-	/	Consistent Negative	SZII
P015	Oropharyngeal swab	Asymptomatic	Close contacts	N/A	>40	>40	-	0.996	-	/	Consistent Negative	SZII
P016	Oropharyngeal swab	Asymptomatic	Close contacts	N/A	>40	>40	-	0.995	-	/	Consistent Negative	SZII
P017	Oropharyngeal swab	Asymptomatic	Close contacts	N/A	>40	>40	-	0.993	-	/	Consistent Negative	SZII

P018	Oropharyngeal swab	Asymptomatic	Close contacts	N/A	>40	>40	-	1.003	-	/	Consistent Negative	SZII
P019	Oropharyngeal swab	Asymptomatic	Close contacts	N/A	>40	>40	-	0.995	-	/	Consistent Negative	SZII
P020	Oropharyngeal swab	Asymptomatic	Close contacts	N/A	>40	>40	-	0.999	-	/	Consistent Negative	SZII
P021	Oropharyngeal swab	Asymptomatic	Close contacts	N/A	>40	>40	-	0.995	-	/	Consistent Negative	SZII
P022	Oropharyngeal swab	Asymptomatic	Close contacts	N/A	>40	>40	-	0.997	-	/	Consistent Negative	SZII
P023	Oropharyngeal swab	Asymptomatic	Close contacts	N/A	>40	>40	-	0.994	-	/	Consistent Negative	SZII
P024	Oropharyngeal swab	Asymptomatic	Close contacts	N/A	>40	>40	-	0.997	-	/	Consistent Negative	SZII
P025	Oropharyngeal swab	Asymptomatic	Close contacts	N/A	>40	>40	-	0.996	-	/	Consistent Negative	SZII
P026	Oropharyngeal swab	Fever, cough	COVID-19 suspected	N/A	18.00	20.00	+	1.447	+	/	Consistent Positive	SZII
P027	Oropharyngeal swab	Fever, cough	COVID-19 suspected	N/A	26.00	27.50	+	1.290	+	/	Consistent Positive	SZII
P028	Oropharyngeal swab	Fever	COVID-19 suspected	N/A	>40	36.09	+	1.386	+	+	Uncertain Positive	SZII
P029	Oropharyngeal swab	Fever	COVID-19 suspected	N/A	>40	35.88	+	1.546	+	+	Uncertain Positive	SZII
P030	Oropharyngeal swab	Asymptomatic	Close contacts	N/A	>40	>40	-	1.015	-	-	Consistent Negative	SZII
P031	Oropharyngeal swab	Asymptomatic	Close contacts	N/A	>40	>40	-	1.017	-	-	Consistent Negative	SZII
P032	Oropharyngeal swab	Fever	COVID-19 suspected	N/A	>40	37.98	+	1.210	+	+	Uncertain Positive	SZII
P033	Oropharyngeal swab	Fever, Dyspnea	Pneumonia	N/A	>40	>40	-	1.024	-	-	Consistent Negative	SZII
P034	Anal swabs	Fever, Dyspnea	Pneumonia	N/A	>40	>40	-	1.012	-	-	Consistent Negative	SZII
P035	Oropharyngeal swab	Fever, Dyspnea	Pneumonia	N/A	>40	>40	-	1.015	-	-	Consistent Negative	SZII
P036	Anal swabs	Fever, Dyspnea	Pneumonia	N/A	>40	>40	-	1.008	-	/	Consistent Negative	SZII
P037	Oropharyngeal swab	Fever, Dyspnea	Pneumonia	N/A	>40	>40	-	1.016	-	-	Consistent Negative	SZII
P038	Anal swabs	Fever, Dyspnea	Pneumonia	N/A	>40	>40	-	1.022	-	-	Consistent Negative	SZII

P039	Oropharyngeal swab	Fever, Dyspnea	Pneumonia	N/A	>40	>40	-	1.014	-	-	Consistent Negative	SZII
P040	Anal swabs	Fever, Dyspnea	Pneumonia	N/A	>40	>40	-	1.014	-	-	Consistent Negative	SZII
P041	Oropharyngeal swab	Fever	COVID-19 suspected	N/A	>40	>40	-	0.994	-	/	Consistent Negative	SZII
P042	Oropharyngeal swab	Fever	COVID-19 suspected	N/A	>40	>40	-	1.011	-	/	Consistent Negative	SZII
P043	Oropharyngeal swab	Fever	COVID-19 suspected	N/A	>40	>40	-	1.006	-	/	Consistent Negative	SZII
P044	Oropharyngeal swab	Fever	COVID-19 suspected	N/A	>40	>40	-	1.018	-	/	Consistent Negative	SZII
P045	Oropharyngeal swab	Fever	COVID-19 suspected	N/A	>40	>40	-	1.000	-	/	Consistent Negative	SZII
P046	Oropharyngeal swab	Fever	COVID-19 suspected	N/A	>40	>40	-	0.988	-	/	Consistent Negative	SZII
P047	Oropharyngeal swab	Fever	COVID-19 suspected	N/A	>40	>40	-	1.014	-	/	Consistent Negative	SZII
P048	Oropharyngeal swab	Fever	COVID-19 suspected	N/A	>40	>40	-	1.002	-	/	Consistent Negative	SZII
P049	Oropharyngeal swab	Fever	COVID-19 suspected	N/A	>40	>40	-	1.010	-	/	Consistent Negative	SZII
P050	Oropharyngeal swab	Fever	COVID-19 suspected	N/A	>40	>40	-	1.006	-	/	Consistent Negative	SZII
P051	Oropharyngeal swab	Fever	COVID-19 suspected	N/A	>40	>40	-	1.004	-	/	Consistent Negative	SZII
P052	Oropharyngeal swab	Fever	COVID-19 suspected	N/A	>40	>40	-	0.998	-	/	Consistent Negative	SZII
P053	Oropharyngeal swab	Fever	COVID-19 suspected	N/A	>40	>40	-	1.016	-	/	Consistent Negative	SZII
P054	Oropharyngeal swab	Fever	COVID-19 suspected	N/A	>40	>40	-	0.998	-	/	Consistent Negative	SZII
P055	Oropharyngeal swab	Fever	COVID-19 suspected	N/A	39.47	>40	Uncertain	0.995	-	-	Uncertain Negative	SZII
P056	Oropharyngeal swab	Fever	COVID-19 suspected	N/A	>40	>40	-	1.024	-	/	Consistent Negative	SZII
P057	Oropharyngeal swab	Fever	COVID-19 suspected	N/A	>40	>40	-	1.008	-	/	Consistent Negative	SZII
P058	Oropharyngeal swab	Fever	COVID-19 suspected	N/A	>40	>40	-	0.998	-	/	Consistent Negative	SZII
P059	Oropharyngeal swab	Fever	COVID-19 suspected	N/A	>40	>40	-	0.995	-	/	Consistent Negative	SZII

P060	Oropharyngeal swab	Fever	COVID-19 suspected	N/A	>40	>40	-	1.014	-	/	Consistent Negative	SZII
P061	Oropharyngeal swab	Fever	COVID-19 suspected	N/A	>40	>40	-	1.010	-	/	Consistent Negative	SZII
P062	Oropharyngeal swab	Fever	COVID-19 suspected	N/A	>40	>40	-	1.008	-	/	Consistent Negative	SZII
P063	Oropharyngeal swab	Fever	COVID-19 suspected	N/A	>40	>40	-	1.007	-	/	Consistent Negative	SZII
P064	Oropharyngeal swab	Fever	COVID-19 suspected	N/A	>40	>40	-	1.005	-	/	Consistent Negative	SZII
P065	Oropharyngeal swab	Fever	COVID-19 suspected	N/A	>40	>40	-	1.016	-	/	Consistent Negative	SZII
P066	Oropharyngeal swab	Fever	COVID-19 suspected	N/A	>40	>40	-	1.001	-	/	Consistent Negative	SZII
P067	Oropharyngeal swab	Fever	COVID-19 suspected	N/A	>40	>40	-	1.001	-	/	Consistent Negative	SZII
P068	Oropharyngeal swab	Fever	COVID-19 suspected	N/A	>40	>40	-	1.009	-	/	Consistent Negative	SZII
P069	Oropharyngeal swab	Fever	COVID-19 suspected	N/A	>40	>40	-	1.005	-	/	Consistent Negative	SZII
P070	Oropharyngeal swab	Fever	COVID-19 suspected	N/A	>40	>40	-	1.009	-	/	Consistent Negative	SZII
P071	Oropharyngeal swab	Fever	COVID-19 suspected	N/A	>40	>40	-	1.003	-	/	Consistent Negative	SZII
P072	Oropharyngeal swab	Fever	COVID-19 suspected	N/A	>40	>40	-	0.952	-	/	Consistent Negative	SZII
P073	Oropharyngeal swab	Fever	COVID-19 suspected	N/A	>40	>40	-	1.009	-	/	Consistent Negative	SZII
P074	Oropharyngeal swab	Fever	COVID-19 suspected	N/A	>40	>40	-	1.004	-	/	Consistent Negative	SZII
P075	Oropharyngeal swab	Fever	COVID-19 suspected	N/A	>40	>40	-	0.992	-	/	Consistent Negative	SZII
P076	Oropharyngeal swab	Fever	COVID-19 suspected	N/A	>40	>40	-	0.992	-	/	Consistent Negative	SZII
P077	Oropharyngeal swab	Fever	COVID-19 suspected	N/A	>40	>40	-	1.000	-	/	Consistent Negative	SZII
P078	Oropharyngeal swab	Fever	COVID-19 suspected	N/A	>40	>40	-	0.996	-	/	Consistent Negative	SZII
P079	Oropharyngeal swab	Fever	COVID-19 suspected	N/A	>40	>40	-	0.995	-	/	Consistent Negative	SZII
P080	Oropharyngeal swab	Fever	COVID-19 suspected	N/A	>40	>40	-	0.987	-	/	Consistent Negative	SZII

P081	Oropharyngeal swab	Fever	COVID-19 suspected	N/A	>40	>40	-	1.009	-	/	Consistent Negative	SZII
P082	Oropharyngeal swab	Fever	COVID-19 suspected	N/A	>40	>40	-	1.010	-	/	Consistent Negative	SZII
P083	Oropharyngeal swab	Fever	COVID-19 suspected	N/A	>40	>40	-	0.999	-	/	Consistent Negative	SZII
P084	Oropharyngeal swab	Fever	COVID-19 suspected	N/A	>40	>40	-	0.983	-	/	Consistent Negative	SZII
P085	Oropharyngeal swab	Fever	COVID-19 suspected	N/A	>40	>40	-	1.011	-	/	Consistent Negative	SZII
P086	Oropharyngeal swab	Fever	COVID-19 suspected	N/A	>40	>40	-	0.986	-	/	Consistent Negative	SZII
P087	Oropharyngeal swab	Fever	COVID-19 suspected	N/A	>40	>40	-	0.990	-	/	Consistent Negative	SZII
P088	Oropharyngeal swab	Fever	COVID-19 suspected	N/A	>40	>40	-	1.002	-	/	Consistent Negative	SZII
P089	Oropharyngeal swab	Fever	COVID-19 suspected	N/A	>40	>40	-	1.002	-	/	Consistent Negative	SZII
P090	Oropharyngeal swab	Fever	COVID-19 suspected	N/A	>40	>40	-	1.001	-	/	Consistent Negative	SZII
P091	Oropharyngeal swab	Fever	COVID-19 suspected	N/A	39.70	>40	Uncertain	0.992	-	-	Uncertain Negative	SZII
P092	Oropharyngeal swab	Fever	COVID-19 suspected	N/A	>40	>40	-	1.001	-	/	Consistent Negative	SZII
P093	Oropharyngeal swab	Fever	COVID-19 suspected	N/A	>40	>40	-	1.004	-	/	Consistent Negative	SZII
P094	Oropharyngeal swab	Fever	COVID-19 suspected	N/A	>40	>40	-	0.999	-	/	Consistent Negative	SZII
P095	Oropharyngeal swab	Fever	COVID-19 suspected	N/A	>40	>40	-	1.008	-	/	Consistent Negative	SZII
P096	Oropharyngeal swab	Fever	COVID-19 suspected	N/A	>40	>40	-	1.006	-	/	Consistent Negative	SZII
P097	Oropharyngeal swab	Fever	COVID-19 suspected	N/A	>40	>40	-	1.003	-	/	Consistent Negative	SZII
P098	Oropharyngeal swab	Fever	COVID-19 suspected	N/A	>40	>40	-	1.010	-	/	Consistent Negative	SZII
P099	Oropharyngeal swab	Fever	COVID-19 suspected	N/A	>40	>40	-	1.001	-	/	Consistent Negative	SZII
P100	Oropharyngeal swab	Fever	COVID-19 suspected	N/A	>40	>40	-	1.006	-	/	Consistent Negative	SZII
P101	Oropharyngeal swab	Fever	COVID-19 suspected	N/A	>40	>40	-	0.997	-	/	Consistent Negative	SZII

P102	Oropharyngeal swab	Fever	COVID-19 suspected	N/A	>40	>40	-	1.004	-	/	Consistent Negative	SZII
P103	Oropharyngeal swab	Fever	COVID-19 suspected	N/A	40.56	>40	Uncertain	0.996	-	-	Uncertain Negative	SZII
P104	Oropharyngeal swab	Fever	COVID-19 suspected	N/A	>40	>40	-	0.988	-	/	Consistent Negative	SZII
P105	Oropharyngeal swab	Fever	COVID-19 suspected	N/A	>40	>40	-	1.001	-	/	Consistent Negative	SZII
P106	Oropharyngeal swab	Fever	COVID-19 suspected	N/A	>40	>40	-	1.002	-	/	Consistent Negative	SZII
P107	Oropharyngeal swab	Fever	COVID-19 suspected	N/A	>40	>40	-	1.000	-	/	Consistent Negative	SZII
P108	Oropharyngeal swab	Fever	COVID-19 suspected	N/A	>40	>40	-	1.008	-	/	Consistent Negative	SZII
P109	Oropharyngeal swab	Fever	COVID-19 suspected	N/A	>40	>40	-	1.005	-	/	Consistent Negative	SZII
P110	Oropharyngeal swab	Fever	COVID-19 suspected	N/A	>40	>40	-	1.031	-	/	Consistent Negative	SZII
P111	Oropharyngeal swab	Fever	COVID-19 suspected	N/A	>40	>40	-	1.004	-	/	Consistent Negative	SZII
P112	Oropharyngeal swab	Fever	COVID-19 suspected	N/A	>40	>40	-	1.008	-	/	Consistent Negative	SZII
P113	Oropharyngeal swab	Fever	COVID-19 suspected	N/A	>40	>40	-	1.013	-	/	Consistent Negative	SZII
P114	Oropharyngeal swab	Fever	COVID-19 suspected	N/A	>40	>40	-	0.994	-	/	Consistent Negative	SZII
P115	Oropharyngeal swab	Fever	COVID-19 suspected	N/A	>40	>40	-	0.998	-	/	Consistent Negative	SZII
P116	Oropharyngeal swab	Fever	COVID-19 suspected	N/A	>40	>40	-	1.000	-	/	Consistent Negative	SZII
P117	Oropharyngeal swab	Fever	COVID-19 suspected	N/A	>40	>40	-	1.000	-	/	Consistent Negative	SZII
P118	Oropharyngeal swab	Fever	COVID-19 suspected	N/A	>40	>40	-	1.005	-	/	Consistent Negative	SZII
P119	Oropharyngeal swab	Fever	COVID-19 suspected	N/A	>40	>40	-	0.992	-	/	Consistent Negative	SZII
P120	Oropharyngeal swab	Fever	COVID-19 suspected	N/A	>40	>40	-	0.981	-	/	Consistent Negative	SZII
P121	Oropharyngeal swab	Fever	COVID-19 suspected	N/A	>40	>40	-	1.015	-	/	Consistent Negative	SZII
P122	Oropharyngeal swab	Fever	COVID-19 suspected	N/A	>40	>40	-	1.001	-	/	Consistent Negative	SZII

P123	Oropharyngeal swab	Fever	COVID-19 suspected	N/A	>40	>40	-	1.001	-	/	Consistent Negative	SZII
P124	Oropharyngeal swab	Fever	COVID-19 suspected	N/A	>40	>40	-	1.003	-	/	Consistent Negative	SZII
P125	Oropharyngeal swab	Fever	COVID-19 suspected	N/A	>40	>40	-	1.000	-	/	Consistent Negative	SZII
P126	Oropharyngeal swab	Fever	COVID-19 suspected	N/A	>40	>40	-	0.987	-	/	Consistent Negative	SZII
P127	Oropharyngeal swab	Fever	COVID-19 suspected	N/A	>40	>40	-	0.994	-	/	Consistent Negative	SZII
P128	Oropharyngeal swab	Fever	COVID-19 suspected	N/A	>40	>40	-	0.989	-	/	Consistent Negative	SZII
P129	Oropharyngeal swab	Fever	COVID-19 suspected	N/A	>40	>40	-	0.978	-	/	Consistent Negative	SZII
P130	Oropharyngeal swab	Fever	COVID-19 suspected	N/A	>40	>40	-	0.991	-	/	Consistent Negative	SZII
P131	Oropharyngeal swab	Fever	COVID-19 suspected	N/A	>40	>40	-	1.001	-	/	Consistent Negative	SZII
P132	Oropharyngeal swab	Fever	COVID-19 suspected	N/A	>40	>40	-	1.001	-	/	Consistent Negative	SZII
P133	Oropharyngeal swab	Fever	COVID-19 suspected	N/A	>40	>40	-	0.998	-	/	Consistent Negative	SZII
P134	Oropharyngeal swab	Fever	COVID-19 suspected	N/A	>40	>40	-	0.995	-	/	Consistent Negative	SZII
P135	Oropharyngeal swab	Fever, cough	COVID-19 suspected	N/A	26.72	26.41	+	1.502	+	/	Consistent Positive	SZII
P136	Oropharyngeal swab	Fever, cough	COVID-19 suspected	N/A	24.38	24.02	+	1.447	+	/	Consistent Positive	SZII
P137	Oropharyngeal swab	Fever, cough	COVID-19 suspected	N/A	38.87	36.28	Uncertain	1.581	+	/	Uncertain Positive	SZII
P138	Oropharyngeal swab	Fever, cough	COVID-19 suspected	N/A	39.22	38.21	Uncertain	1.609	+	/	Uncertain Positive	SZII
P139	Oropharyngeal swab	Fever, cough	COVID-19 suspected	N/A	36.26	33.90	+	1.646	+	/	Consistent Positive	SZII
P140-1	Throat swab	No common respiratory symptoms	Came from Wuhan, suspected	N/A	>40	>40	-	0.992	-	/	Consistent Negative	DF
P140-2	Nasopharyngeal swab (Left)	No common respiratory symptoms	Came from Wuhan, suspected	N/A	>40	>40	-	1.003	-	/	Consistent Negative	DF
P140-3	Nasopharyngeal swab (Right)	No common respiratory symptoms	Came from Wuhan, suspected	N/A	35.96	37.24	+	1.430	+	+	Consistent Positive	DF

P140-4	Blood serum	No common respiratory symptoms	Came from Wuhan, suspected	N/A	>40	>40	-	1.002	-	/	Consistent Negative	DF
P140-5	Nasopharyngeal swab	No common respiratory symptoms	Came from Wuhan, suspected	N/A	>40	>40	-	1.006	-	/	Consistent Negative	DF
P140-6	Nasol swab	No common respiratory symptoms	Came from Wuhan, suspected	N/A	>40	>40	-	1.614	+	+	False Negative	DF
P140-7	Nasol swab	No common respiratory symptoms	Came from Wuhan, suspected	N/A	>40	>40	-	1.369	+	+	False Negative	DF
P140-8	Blood serum	No common respiratory symptoms	Came from Wuhan, suspected	N/A	>40	>40	-	1.000	-	/	Consistent Negative	DF
P140-9	Nasopharyngeal swab (Left)	No common respiratory symptoms	Came from Wuhan, suspected	N/A	>40	>40	-	1.004	-	-	Consistent Negative	DF
P140-10	Nasopharyngeal swab (Right)	No common respiratory symptoms	Came from Wuhan, suspected	N/A	>40	>40	-	1.004	-	/	Consistent Negative	DF
P140-11	Throat swab	No common respiratory symptoms	Came from Wuhan, suspected	N/A	>40	>40	-	1.002	-	/	Consistent Negative	DF
P140-12	Serum	No common respiratory symptoms	Came from Wuhan, suspected	N/A	>40	>40	-	1.007	-	/	Consistent Negative	DF
P140-13	Plasma	No common respiratory symptoms	Came from Wuhan, suspected	N/A	>40	>40	-	1.005	-	/	Consistent Negative	DF
P140-14	Fecal	No common respiratory symptoms	Came from Wuhan, suspected	N/A	>40	>40	-	1.002	-	/	Consistent Negative	DF
P141	Nasopharyngeal swab	Fever	COVID-19 suspected	32.68	33.98	33.42	+	1.673	+	+	Consistent Positive	RJ
P142	Nasopharyngeal swab	Fever	COVID-19 suspected	35.76	37.54	36.28	+	1.391	+	+	Consistent Positive	RJ
P143	Nasopharyngeal swab	Fever, Chest pain	COVID-19 suspected	>45	>45	>45	-	1.245	+	+	False Negative	RJ
P144	Nasopharyngeal swab	Cough	Upper respiratory infection	41.92	>45	>45	Uncertain	1.022	-	-	Uncertain Negative	RJ
P145	Nasopharyngeal swab	Fever	Upper respiratory infection	41.42	>45	>45	Uncertain	0.897	-	-	Uncertain Negative	RJ

P146	Nasopharyngeal swab	Chest pain	COVID-19 suspected	42.62	>45	>45	Uncertain	0.898	-	-	Uncertain Negative	RJ
P147	Nasopharyngeal swab	Cough	Upper respiratory infection	41.34	>45	>45	Uncertain	0.730	-	-	Uncertain Negative	RJ
P148	Nasopharyngeal swab	Fever	COVID-19 suspected	42.89	>45	>45	Uncertain	0.812	-	-	Uncertain Negative	RJ
P149	Nasopharyngeal swab	Dyspnea	Pneumonia	42.65	>45	>45	Uncertain	0.768	-	-	Uncertain Negative	RJ
P150	Nasopharyngeal swab	Fever	COVID-19 suspected	41.82	>45	>45	Uncertain	0.991	-	-	Uncertain Negative	RJ
P151	Nasopharyngeal swab	Asymptomatic	Upper respiratory infection	42.14	>45	>45	Uncertain	0.960	-	-	Uncertain Negative	RJ
P152	Nasopharyngeal swab	Dyspnea	COVID-19 suspected	41.74	>45	>45	Uncertain	0.960	-	-	Uncertain Negative	RJ
P153	Nasopharyngeal swab	Fever	Upper respiratory infection	41.84	>45	>45	Uncertain	0.897	-	-	Uncertain Negative	RJ
P154	Nasopharyngeal swab	Chest pain	Heart failure	42.04	>45	>45	Uncertain	0.991	-	-	Uncertain Negative	RJ
P155	Nasopharyngeal swab	cough	Pneumonia	41.12	>45	>45	Uncertain	0.898	-	-	Uncertain Negative	RJ
P156	Nasopharyngeal swab	Fever	Pneumonia	>45	>45	>45	-	0.936	-	/	Consistent Negative	RJ
P157	Nasopharyngeal swab	Cough	Upper respiratory infection	>45	>45	>45	-	0.894	-	/	Consistent Negative	RJ
P158	Nasopharyngeal swab	Fever	COVID-19 suspected	>45	>45	>45	-	0.970	-	/	Consistent Negative	RJ
P159	Nasopharyngeal swab	Fever	COVID-19 suspected	44.62	>45	>45	-	0.870	-	/	Consistent Negative	RJ
P160	Nasopharyngeal swab	Dyspnea	Diabetes	>45	>45	>45	-	0.817	-	/	Consistent Negative	RJ
P161	Nasopharyngeal swab	Cough	Upper respiratory infection	>45	>45	>45	-	0.804	-	/	Consistent Negative	RJ
P162	Nasopharyngeal swab	Fever	Diabetes	>45	>45	>45	-	0.859	-	/	Consistent Negative	RJ
P163	Nasopharyngeal swab	Dyspnea	Upper respiratory infection	>45	>45	>45	-	0.815	-	/	Consistent Negative	RJ
P164	Nasopharyngeal swab	Fever	Upper respiratory infection	>45	>45	>45	-	0.871	-	/	Consistent Negative	RJ
P165	Nasopharyngeal swab	Cough	Diabetes	>45	>45	>45	-	0.802	-	/	Consistent Negative	RJ
P166	Nasopharyngeal swab	Cough	Diabetes	>45	>45	>45	-	0.990	-	/	Consistent Negative	RJ

P167	Nasopharyngeal swab	Fever	Upper respiratory infection	>45	>45	>45	-	0.817	-	/	Consistent Negative	RJ
P168	Nasopharyngeal swab	Fever	Diabetes	>45	>45	>45	-	0.760	-	/	Consistent Negative	RJ
P169	Nasopharyngeal swab	Dyspnea	Upper respiratory infection	>45	>45	>45	-	0.802	-	/	Consistent Negative	RJ
P170	Nasopharyngeal swab	Asymptomatic	Close contacts	>45	>45	>45	-	0.636	-	/	Consistent Negative	RJ
P171	Nasopharyngeal swab	Fever	Upper respiratory infection	>45	>45	>45	-	0.758	-	/	Consistent Negative	RJ
P172	Nasopharyngeal swab	Fever	Upper respiratory infection	43.12	>45	>45	-	0.931	-	/	Consistent Negative	RJ
P173	Nasopharyngeal swab	Chest pain	Pneumonia	>45	>45	>45	-	0.758	-	/	Consistent Negative	RJ
P174	Nasopharyngeal swab	Fever	Diabetes	>45	>45	>45	-	0.951	-	/	Consistent Negative	RJ
P175	Nasopharyngeal swab	Cough	Upper respiratory infection	>45	>45	>45	-	0.974	-	/	Consistent Negative	RJ
P176	Nasopharyngeal swab	Chest pain	Pneumonia	>45	>45	>45	-	0.683	-	/	Consistent Negative	RJ
P177	Nasopharyngeal swab	Dyspnea	Upper respiratory infection	43.65	>45	>45	-	0.959	-	/	Consistent Negative	RJ
P178	Nasopharyngeal swab	Cough	Upper respiratory infection	>45	>45	>45	-	0.926	-	/	Consistent Negative	RJ
P179	Nasopharyngeal swab	Fever	COVID-19 suspected	44.12	>45	>45	-	0.761	-	/	Consistent Negative	RJ
P180	Nasopharyngeal swab	Fever	COVID-19 suspected	>45	>45	>45	-	0.685	-	/	Consistent Negative	RJ
P181	Nasopharyngeal swab	Fever	Upper respiratory infection	>45	>45	>45	-	0.815	-	/	Consistent Negative	RJ
P182	Nasopharyngeal swab	Asymptomatic	Close contacts	>45	>45	>45	-	0.943	-	/	Consistent Negative	RJ
P183	Nasopharyngeal swab	Dyspnea	Pneumonia	>45	>45	>45	-	0.850	-	/	Consistent Negative	RJ
P184	Nasopharyngeal swab	Cough	Upper respiratory infection	>45	>45	>45	-	0.758	-	/	Consistent Negative	RJ
P185	Nasopharyngeal swab	Fever	Upper respiratory infection	>45	>45	>45	-	0.582	-	/	Consistent Negative	RJ
P186	Nasopharyngeal swab	Cough	Upper respiratory infection	>45	>45	>45	-	0.655	-	/	Consistent Negative	RJ
P187	Nasopharyngeal swab	Cough	Upper respiratory infection	>45	>45	>45	-	0.936	-	/	Consistent Negative	RJ

P188	Nasopharyngeal swab	Fever	Pneumonia	>45	>45	>45	-	0.647	-	/	Consistent Negative	RJ
P189	Nasopharyngeal swab	Fever	Upper respiratory infection	>45	>45	>45	-	0.699	-	/	Consistent Negative	RJ
P190	Nasopharyngeal swab	Fever	Pneumonia	>45	>45	>45	-	0.994	-	/	Consistent Negative	RJ
P191	Nasopharyngeal swab	Fever	Upper respiratory infection	>45	>45	>45	-	0.764	-	/	Consistent Negative	RJ
P192	Nasopharyngeal swab	Fever	Upper respiratory infection	>45	>45	>45	-	0.626	-	/	Consistent Negative	RJ
P193	Nasopharyngeal swab	Cough	Diabetes	>45	>45	>45	-	0.800	-	/	Consistent Negative	RJ
P194	Nasopharyngeal swab	Fever	Upper respiratory infection	>45	>45	>45	-	0.674	-	/	Consistent Negative	RJ
P195	Nasopharyngeal swab	Dyspnea	Pneumonia	>45	>45	>45	-	0.589	-	/	Consistent Negative	RJ
P196	Nasopharyngeal swab	Fever	Upper respiratory infection	>45	>45	>45	-	0.580	-	/	Consistent Negative	RJ
P197	Nasopharyngeal swab	Fever	Upper respiratory infection	>45	>45	>45	-	0.630	-	/	Consistent Negative	RJ
P198	Nasopharyngeal swab	Asymptomatic	Close contacts	>45	>45	>45	-	0.846	-	/	Consistent Negative	RJ
P199	Nasopharyngeal swab	Fever	Upper respiratory infection	>45	>45	>45	-	0.644	-	/	Consistent Negative	RJ
P200	Nasopharyngeal swab	Fever	Upper respiratory infection	>45	>45	>45	-	0.760	-	/	Consistent Negative	RJ
P201	Nasopharyngeal swab	Cough	Pneumonia	>45	>45	>45	-	0.949	-	/	Consistent Negative	RJ
P202	Nasopharyngeal swab	Fever	Upper respiratory infection	>45	>45	>45	-	0.905	-	/	Consistent Negative	RJ
P203	Nasopharyngeal swab	Fever	Pneumonia	>45	>45	>45	-	0.799	-	/	Consistent Negative	RJ
P204	Nasopharyngeal swab	Fever	Pneumonia	>45	>45	>45	-	0.905	-	/	Consistent Negative	RJ
P205	Nasopharyngeal swab	Asymptomatic	Close contacts	>45	>45	>45	-	0.868	-	/	Consistent Negative	RJ
P206	Nasopharyngeal swab	Fever	Upper respiratory infection	>45	>45	>45	-	0.674	-	/	Consistent Negative	RJ
P207	Nasopharyngeal swab	Asymptomatic	Close contacts	>45	>45	>45	-	0.936	-	/	Consistent Negative	RJ
P208	Nasopharyngeal swab	Chest pain	Pneumonia	>45	>45	>45	-	0.802	-	/	Consistent Negative	RJ

P209	Nasopharyngeal swab	Fever	Upper respiratory infection	>45	>45	>45	-	0.630	-	/	Consistent Negative	RJ
P210	Nasopharyngeal swab	Fever	COVID-19 suspected	>45	>45	>45	-	0.737	-	/	Consistent Negative	RJ
P211	Nasopharyngeal swab	Fever	COVID-19 suspected	>45	>45	>45	-	0.905	-	/	Consistent Negative	RJ
P212	Nasopharyngeal swab	Fever	Upper respiratory infection	>45	>45	>45	-	0.999	-	/	Consistent Negative	RJ
P213	Nasopharyngeal swab	Fever	Upper respiratory infection	>45	>45	>45	-	0.942	-	/	Consistent Negative	RJ
P214	Nasopharyngeal swab	Cough	Diabetes	>45	>45	>45	-	0.848	-	/	Consistent Negative	RJ
P215	Nasopharyngeal swab	Cough	Upper respiratory infection	>45	>45	>45	-	0.772	-	/	Consistent Negative	RJ
P216	Nasopharyngeal swab	Cough	Upper respiratory infection	>45	>45	>45	-	0.948	-	/	Consistent Negative	RJ
P217	Nasopharyngeal swab	Fever	Upper respiratory infection	>45	>45	>45	-	0.848	-	/	Consistent Negative	RJ
P218	Nasopharyngeal swab	Fever	Diabetes	>45	>45	>45	-	0.816	-	/	Consistent Negative	RJ
P219	Nasopharyngeal swab	Fever	Upper respiratory infection	>45	>45	>45	-	0.759	-	/	Consistent Negative	RJ
P220	Nasopharyngeal swab	Fever	COVID-19 suspected	>45	>45	>45	-	0.825	-	/	Consistent Negative	RJ
P221	Nasopharyngeal swab	Chest pain	Heart failure	>45	>45	>45	-	0.807	-	/	Consistent Negative	RJ
P222	Nasopharyngeal swab	Fever	Upper respiratory infection	>45	>45	>45	-	0.654	-	/	Consistent Negative	RJ
P223	Nasopharyngeal swab	Asymptomatic	Close contacts	>45	>45	>45	-	0.931	-	/	Consistent Negative	RJ
P224	Nasopharyngeal swab	Fever	Upper respiratory infection	>45	>45	>45	-	0.973	-	/	Consistent Negative	RJ
P225	Nasopharyngeal swab	Fever	Upper respiratory infection	>45	>45	>45	-	0.985	-	/	Consistent Negative	RJ
P226	Nasopharyngeal swab	Fever	Upper respiratory infection	>45	>45	>45	-	1.027	-	/	Consistent Negative	RJ
P227	Nasopharyngeal swab	Asymptomatic	Close contacts	>45	>45	>45	-	1.011	-	/	Consistent Negative	RJ
P228	Nasopharyngeal swab	Fever	Upper respiratory infection	44.18	>45	>45	-	1.049	-	/	Consistent Negative	RJ
P229	Nasopharyngeal swab	Fever	Diabetes	>45	>45	>45	-	0.970	-	/	Consistent Negative	RJ

P230	Nasopharyngeal swab	Fever	Upper respiratory infection	>45	>45	>45	-	0.921	-	/	Consistent Negative	RJ
P231	Nasopharyngeal swab	Fever	COVID-19 suspected	>45	>45	>45	-	0.906	-	/	Consistent Negative	RJ
P232	Nasopharyngeal swab	Fever	Upper respiratory infection	>45	>45	>45	-	1.082	-	/	Consistent Negative	RJ
P233	Nasopharyngeal swab	Dyspnea	Pneumonia	>45	>45	>45	-	1.027	-	/	Consistent Negative	RJ
P234	Nasopharyngeal swab	Cough	Upper respiratory infection	>45	>45	>45	-	0.926	-	/	Consistent Negative	RJ
P235	Nasopharyngeal swab	Fever	Upper respiratory infection	>45	>45	>45	-	0.985	-	/	Consistent Negative	RJ
P236	Nasopharyngeal swab	Fever	COVID-19 suspected	>45	>45	>45	-	0.985	-	/	Consistent Negative	RJ
P237	Nasopharyngeal swab	Chest pain	Heart failure	>45	>45	>45	-	1.049	-	/	Consistent Negative	RJ
P238	Nasopharyngeal swab	Fever	Upper respiratory infection	>45	>45	>45	-	1.032	-	/	Consistent Negative	RJ
P239	Nasopharyngeal swab	Asymptomatic	Close contacts	>45	>45	>45	-	1.082	-	/	Consistent Negative	RJ
P240	Nasopharyngeal swab	Asymptomatic	Close contacts	>45	>45	>45	-	0.989	-	/	Consistent Negative	RJ
P241	Nasopharyngeal swab	Fever	Upper respiratory infection	>45	>45	>45	-	1.049	-	/	Consistent Negative	RJ
P242	Nasopharyngeal swab	Cough	Upper respiratory infection	>45	>45	>45	-	1.049	-	/	Consistent Negative	RJ
P243	Nasopharyngeal swab	Asymptomatic	Close contacts	>45	>45	>45	-	0.906	-	/	Consistent Negative	RJ
P244	Nasopharyngeal swab	Cough	Upper respiratory infection	>45	>45	>45	-	0.921	-	/	Consistent Negative	RJ
P245	Nasopharyngeal swab	Fever	Upper respiratory infection	>45	>45	>45	-	0.843	-	/	Consistent Negative	RJ
P246	Nasopharyngeal swab	Fever	Upper respiratory infection	>45	>45	>45	-	0.936	-	/	Consistent Negative	RJ
P247	Nasopharyngeal swab	Fever	Diabetes	>45	>45	>45	-	1.035	-	/	Consistent Negative	RJ
P248	Nasopharyngeal swab	Asymptomatic	Close contacts	>45	>45	>45	-	0.936	-	/	Consistent Negative	RJ
P249	Nasopharyngeal swab	Asymptomatic	Close contacts	>45	>45	>45	-	0.906	-	/	Consistent Negative	RJ
P250	Nasopharyngeal swab	Fever	COVID-19 suspected	>45	>45	>45	-	1.066	-	/	Consistent Negative	RJ

P251	Nasopharyngeal swab	Asymptomatic	Close contacts	>45	>45	>45	-	0.950	-	/	Consistent Negative	RJ
P252	Nasopharyngeal swab	Dyspnea	Upper respiratory infection	>45	>45	>45	-	0.970	-	/	Consistent Negative	RJ
P253	Nasopharyngeal swab	Asymptomatic	Close contacts	>45	>45	>45	-	0.921	-	/	Consistent Negative	RJ
P254	Nasopharyngeal swab	Cough	Upper respiratory infection	>45	>45	>45	-	1.027	-	/	Consistent Negative	RJ
P255	Nasopharyngeal swab	Fever	Upper respiratory infection	>45	>45	>45	-	1.032	-	/	Consistent Negative	RJ
P256	Nasopharyngeal swab	Fever	COVID-19 suspected	>45	>45	>45	-	0.936	-	/	Consistent Negative	RJ
P257	Nasopharyngeal swab	Asymptomatic	Close contacts	>45	>45	>45	-	0.901	-	/	Consistent Negative	RJ
P258	Nasopharyngeal swab	Fever	Upper respiratory infection	>45	>45	>45	-	0.950	-	/	Consistent Negative	RJ
P259	Nasopharyngeal swab	Asymptomatic	Close contacts	>45	>45	>45	-	1.027	-	/	Consistent Negative	RJ
P260	Nasopharyngeal swab	Cough	Upper respiratory infection	>45	>45	>45	-	1.066	-	/	Consistent Negative	RJ
P261	Nasopharyngeal swab	Fever	Upper respiratory infection	>45	>45	>45	-	0.911	-	/	Consistent Negative	RJ
P262	Nasopharyngeal swab	Asymptomatic	Close contacts	>45	>45	>45	-	0.936	-	/	Consistent Negative	RJ
P263	Nasopharyngeal swab	Asymptomatic	Close contacts	>45	>45	>45	-	0.921	-	/	Consistent Negative	RJ
P264	Nasopharyngeal swab	Cough	Upper respiratory infection	>45	>45	>45	-	1.066	-	/	Consistent Negative	RJ
P265	Nasopharyngeal swab	Asymptomatic	Close contacts	>45	>45	>45	-	0.901	-	/	Consistent Negative	RJ
P266	Nasopharyngeal swab	Fever	Upper respiratory infection	>45	>45	>45	-	0.936	-	/	Consistent Negative	RJ
P267	Nasopharyngeal swab	Asymptomatic	Close contacts	43.65	>45	>45	-	0.936	-	/	Consistent Negative	RJ
P268	Nasopharyngeal swab	Cough	Upper respiratory infection	>45	>45	>45	-	1.027	-	/	Consistent Negative	RJ
P269	Nasopharyngeal swab	Fever	Upper respiratory infection	>45	>45	>45	-	0.921	-	/	Consistent Negative	RJ
P270	Nasopharyngeal swab	Cough	Upper respiratory infection	>45	>45	>45	-	1.066	-	/	Consistent Negative	RJ
P271	Nasopharyngeal swab	Asymptomatic	Close contacts	>45	>45	>45	-	1.027	-	/	Consistent Negative	RJ

P272	Nasopharyngeal swab	Dyspnea	Pneumonia	>45	>45	>45	-	0.904	-	/	Consistent Negative	RJ
P273	Nasopharyngeal swab	Cough	Upper respiratory infection	>45	>45	>45	-	1.082	-	/	Consistent Negative	RJ
P274	Nasopharyngeal swab	Fever	Diabetes	>45	>45	>45	-	0.936	-	/	Consistent Negative	RJ
P275	Nasopharyngeal swab	Asymptomatic	Close contacts	>45	>45	>45	-	1.066	-	/	Consistent Negative	RJ
P276	Nasopharyngeal swab	Asymptomatic	Close contacts	>45	>45	>45	-	1.011	-	/	Consistent Negative	RJ
P277	Nasopharyngeal swab	Asymptomatic	Close contacts	>45	>45	>45	-	0.877	-	/	Consistent Negative	RJ
P278-1	Nasopharyngeal swab	Asymptomatic	Close contacts	N/A	36.25	N/A	+	1.068	-	-	False Positive	RJ
P278-2	Nasopharyngeal swab	Asymptomatic	Close contacts	>45	>45	>45	-	1.068	-	/	Consistent Negative	RJ
P279-1	Nasopharyngeal swab	Asymptomatic	Close contacts	N/A	36.89	N/A	+	1.030	-	-	False Positive	RJ
P279-2	Nasopharyngeal swab	Asymptomatic	Close contacts	>45	>45	>45	-	1.030	-	/	Consistent Negative	RJ
P280	Oropharyngeal swab	Fever, Cough, Headache	COVID-19 suspected	N/A	>40	34.27	Uncertain	1.172	+	/	Uncertain Positive	JNCDC
P281	Fecal	Fever, Cough, Rhinobyon	Close contacts	N/A	30.20	30.46	+	1.453	+	/	Consistent Positive	JNCDC
P282	Fecal	Fever, Cough, Rhinobyon	COVID-19 suspected	N/A	38.50	>40	-	1.250	+	/	False Negative	JNCDC

Note: N/A, Detection of this gene that was not supported by the kit. “+”, Positive; “-”, negative; /, PCR product was not analyzed by NGS. Samples in aquamarine background stood for SENA negative but rRT-PCR positive or uncertain diagnosis. Samples in red background stood for SENA positive but rRT-PCR negative or uncertain diagnosis.

References

1. F. Wu, S. Zhao, B. Yu, Y. M. Chen, W. Wang, Z. G. Song, Y. Hu, Z. W. Tao, J. H. Tian, Y. Y. Pei, M. L. Yuan, Y. L. Zhang, F. H. Dai, Y. Liu, Q. M. Wang, J. J. Zheng, L. Xu, E. C. Holmes, Y. Z. Zhang, A new coronavirus associated with human respiratory disease in China. *Nature* **579**, 265-269 (2020). doi: [10.1038/s41586-020-2008-3](https://doi.org/10.1038/s41586-020-2008-3).
2. W. H. Organization, Coronavirus disease 2019 (COVID-19) Situation Report-132. Available at: <https://www.who.int/emergencies/diseases/novel-coronavirus-2019/situation-reports/>. Last accessed, May 31, 2020.
3. V. M. Corman, O. Landt, M. Kaiser, R. Molenkamp, A. Meijer, D. K. Chu, T. Bleicker, S. Brunink, J. Schneider, M. L. Schmidt, D. G. Mulders, B. L. Haagmans, B. van der Veer, S. van den Brink, L. Wijsman, G. Goderski, J. L. Romette, J. Ellis, M. Zambon, M. Peiris, H. Goossens, C. Reusken, M. P. Koopmans, C. Drosten, Detection of 2019 novel coronavirus (2019-nCoV) by real-time RT-PCR. *Euro surveillance*, **25**, (2020). doi: [10.2807/1560-7917.ES.2020.25.3.2000045](https://doi.org/10.2807/1560-7917.ES.2020.25.3.2000045).
4. H. Feng, Y. Liu, M. Lv, J. Zhong, A case report of COVID-19 with false negative RT-PCR test: necessity of chest CT. *Jpn J Radiol*, (2020). doi: [10.1007/s11604-020-00967-9](https://doi.org/10.1007/s11604-020-00967-9).
5. Y. Li, L. Yao, J. Li, L. Chen, Y. Song, Z. Cai, C. Yang, Stability issues of RT-PCR testing of SARS-CoV-2 for hospitalized patients clinically diagnosed with COVID-19. *Journal of medical virology*, (2020). doi: [10.1002/jmv.25786](https://doi.org/10.1002/jmv.25786).
6. Y. Pan, L. Long, D. Zhang, T. Yan, S. Cui, P. Yang, Q. Wang, S. Ren, Potential false-negative nucleic acid testing results for Severe Acute Respiratory Syndrome Coronavirus 2 from thermal inactivation of samples with low viral loads. *Clin Chem*, (2020). doi: [10.1093/clinchem/hvaa091](https://doi.org/10.1093/clinchem/hvaa091).
7. J. Wu, J. Liu, S. Li, Z. Peng, Z. Xiao, X. Wang, R. Yan, J. Luo, Detection and analysis of nucleic acid in various biological samples of COVID-19 patients. *Travel medicine and infectious disease*, 101673 (2020). doi: [10.1016/j.tmaid.2020.101673](https://doi.org/10.1016/j.tmaid.2020.101673).
8. A. T. Xiao, Y. X. Tong, S. Zhang, False-negative of RT-PCR and prolonged nucleic acid conversion in COVID-19: Rather than recurrence. *Journal of medical virology*, (2020). doi: [10.1002/jmv.25855](https://doi.org/10.1002/jmv.25855).
9. J. S. Gootenberg, O. O. Abudayyeh, J. W. Lee, P. Essletzbichler, A. J. Dy, J. Joung, V. Verdine, N. Donghia, N. M. Daringer, C. A. Freije, C. Myhrvold, R. P. Bhattacharyya, J. Livny, A. Regev, E. V. Koonin, D. T. Hung, P. C. Sabeti, J. J. Collins, F. Zhang, Nucleic acid detection with CRISPR-Cas13a/C2c2. *Science* **356**, 438-442 (2017). doi: [10.1126/science.aam9321](https://doi.org/10.1126/science.aam9321).
10. J. S. Gootenberg, O. O. Abudayyeh, M. J. Kellner, J. Joung, J. J. Collins, F. Zhang, Multiplexed and portable nucleic acid detection platform with Cas13, Cas12a, and Csm6. *Science* **360**, 439 (2018). doi: [10.1126/science.aag0179](https://doi.org/10.1126/science.aag0179).
11. S. Y. Li, Q. X. Cheng, J. K. Liu, X. Q. Nie, G. P. Zhao, J. Wang, CRISPR-Cas12a has both cis- and trans-cleavage activities on single-stranded DNA. *Cell research* **28**, 491-493 (2018). doi: [10.1038/s41422-018-0022-x](https://doi.org/10.1038/s41422-018-0022-x).
12. J. S. Chen, E. Ma, L. B. Harrington, M. Da Costa, X. Tian, J. M. Palefsky, J. A. Doudna, CRISPR-Cas12a target binding unleashes indiscriminate single-stranded DNase activity. *Science* **360**, 436-439 (2018). doi: [10.1126/science.aar6245](https://doi.org/10.1126/science.aar6245).
13. L. B. Harrington, D. Burstein, J. S. Chen, D. Paez-Espino, E. Ma, I. P. Witte, J. C. Cofsky, N. C. Kyrpides, J. F. Banfield, J. A. Doudna, Programmed DNA destruction by miniature CRISPR-Cas14 enzymes. *Science* **362**, 839-842 (2018). doi: [10.1126/science.aav4294](https://doi.org/10.1126/science.aav4294).
14. L. Li, S. Li, N. Wu, J. Wu, G. Wang, G. P. Zhao, J. Wang, HOLMESv2: a CRISPR-Cas12b-assisted platform for nucleic acid detection and DNA methylation quantitation. *ACS Synth Biol*, (2019). doi: [10.1021/acssynbio.9b00209](https://doi.org/10.1021/acssynbio.9b00209).
15. D. S. Chertow, Next-generation diagnostics with CRISPR. *Science* **360**, 381-382 (2018). doi: [10.1126/science.aat4982](https://doi.org/10.1126/science.aat4982).
16. G. Gasiunas, R. Barrangou, P. Horvath, V. Siksnys, Cas9-crRNA ribonucleoprotein complex mediates specific DNA cleavage for adaptive immunity in bacteria. *Proceedings of the National Academy of Sciences of the United States of America* **109**, E2579-2586 (2012). doi: [10.1073/pnas.1208507109](https://doi.org/10.1073/pnas.1208507109).
17. M. Jinek, K. Chylinski, I. Fonfara, M. Hauer, J. A. Doudna, E. Charpentier, A programmable dual-RNA-guided DNA endonuclease in adaptive bacterial immunity. *Science* **337**, 816-821 (2012). doi: [10.1126/science.1225829](https://doi.org/10.1126/science.1225829).
18. S. Y. Li, Q. X. Cheng, J. M. Wang, X. Y. Li, Z. L. Zhang, S. Gao, R. B. Cao, G. P. Zhao, J. Wang, CRISPR-Cas12a-assisted nucleic acid detection. *Cell discovery* **4**, 20 (2018). doi: [10.1038/s41421-018-0028-z](https://doi.org/10.1038/s41421-018-0028-z).
19. S. A. Bustin, T. Nolan, Pitfalls of quantitative real-time reverse-transcription polymerase chain reaction. *Journal of biomolecular techniques: JBT* **15**, 155-66 (2004).
20. M. Burns, H. Valdivia, Modelling the limit of detection in real-time quantitative PCR. *European Food Research and Technology* **226**, 1513-1524 (2007). doi: [10.1007/s00217-007-0683-z](https://doi.org/10.1007/s00217-007-0683-z).

21. A. Forootan, R. Sjoback, J. Bjorkman, B. Sjogreen, L. Linz, M. Kubista, Methods to determine limit of detection and limit of quantification in quantitative real-time PCR (qPCR). *Biomolecular detection and quantification* **12**, 1-6 (2017). doi: [10.1016/j.bdq.2017.04.001](https://doi.org/10.1016/j.bdq.2017.04.001).
22. W. Fu, Q. Chen, T. Wang, Letter to the Editor: Three cases of re-detectable positive SARS-CoV-2 RNA in recovered COVID-19 patients with antibodies. *Journal of medical virology*, (2020). doi: [10.1002/jmv.25968](https://doi.org/10.1002/jmv.25968)
23. B. Langmead, S. L. Salzberg, Fast gapped-read alignment with Bowtie 2. *Nature methods* **9**, 357-359 (2012). doi: [10.1038/nmeth.1923](https://doi.org/10.1038/nmeth.1923).
24. W. Z. Tieying Hou, Minling Yang, Wenjing Chen, Lili Ren, Jingwen Ai , Ji Wu, Yalong Liao, Xuejing Gou, Yongjun Li, Xiaorui Wang, Hang Su, Bing Gu, Jianwei Wang, Teng Xu, Development and Evaluation of A CRISPR-based Diagnostic For 2019-novel Coronavirus. *medRxiv* [preprint]. (2020). doi:[10.1101/2020.02.22.20025460](https://doi.org/10.1101/2020.02.22.20025460).